APPLICATION OF VERY HIGH RESOLUTION IMAGERY AND TERRESTRIAL LASER SCANNING FOR ESTIMATING CARBON STOCK IN TROPICAL RAIN FOREST OF ROYAL BELUM, MALAYSIA

MEBRAT TIKABO SIUM
February, 2015

SUPERVISORS:
Dr. Y.A. Hussin
Dr. M.J.C. Wier

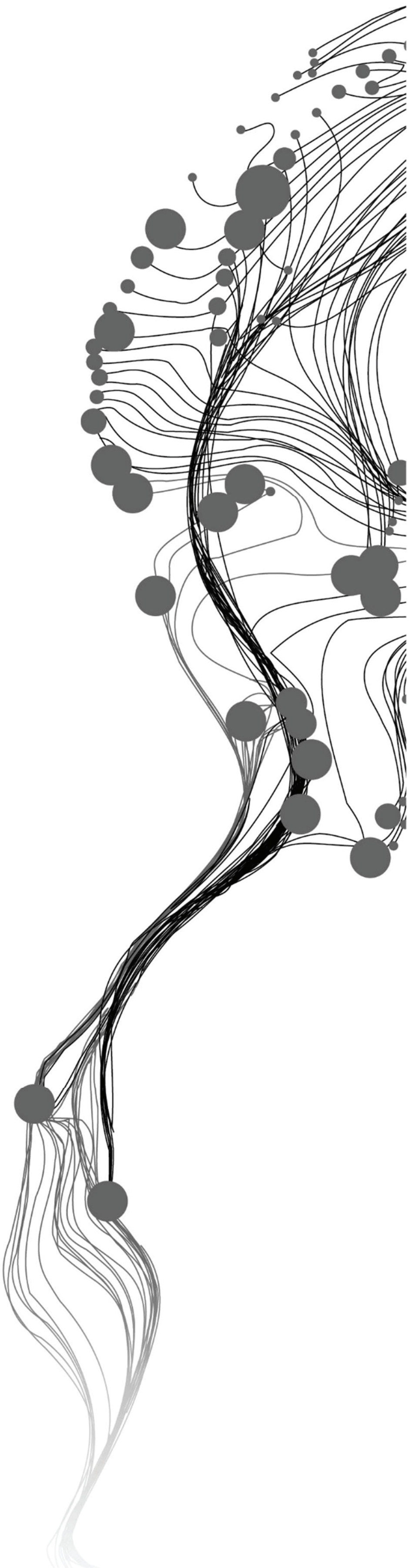

APPLICATION OF VERY HIGH RESOLUTION IMAGERY AND TERRESTRIAL LASER SCANNING FOR ESTIMATING CARBON STOCK IN TROPICAL RAIN FOREST OF ROYAL BELUM, MALAYSIA

MEBRAT TIKABO SIUM
Enschede, The Netherlands, February, 2015

Thesis submitted to the Faculty of Geo-Information Science and Earth Observation of the University of Twente in partial fulfilment of the requirements for the degree of Master of Science in Geo-information Science and Earth Observation.
Specialization: Natural Resources Management

SUPERVISORS:
Dr. Y. A. Hussin
Dr. M.J.C. Weir

THESIS ASSESSMENT BOARD:
Dr. Ir. C. A. J. M. de Bie (Chairman)
Dr. T. Kauranne (External Examiner, Arbonaut Oy Ltd. And Department of Mathematics and Physics-Lappeenranta University of Technology, Finland)

ABSTRACT

Forests are one of the most important resources which continue to be exploited at an alarming rate resulting in their deforestation and degradation and associated carbon emission. Under UNFCCC and Kyoto Protocol, reducing emission from deforestation and forest degradation (REDD) and its Measuring Reporting and Verifying (MRV) mechanism was implemented to mitigate climate change through reduced carbon emission from deforestation and forest degradation. Thus all countries committed to reduce emission or remove greenhouse gases through enhanced forest management under REDD+ mechanism should update the inventories of estimated carbon stock in their forests. However, an accurate method of estimating forest carbon stock is a challenge.

In this study combination of extracted data from Terrestrial Laser Scanner (TLS) and WorldView-2, a very high resolution image was used to develop an accurate method of estimating above ground carbon stock. The total above ground biomass (AGB) was calculated using allometric equation from DBH and height derived from TLS, which was then converted to carbon using conversion factor of 0.47. Object Base Image analysis was applied to accurately segment crown projection area (CPA) from a very high resolution satellite image. A relationship was then established between DBH and height from TLS and CPA from image using 71 trees. These 71 trees are those recognized from high resolution image and matched as one to one to their ground reference polygons and detected from point cloud data. Field measured and TLS derived DBH and height were compared hence, both DBH and height extracted from TLS were not significantly different from field measurement at 95% confidence level. Correlation analysis among independent variables of above ground carbon estimation (CPA, DBH, height) was carried out. The independent variables were also correlated with dependent variable (carbon). A non-linear regression model was developed between calculated carbon and CPA derived from image to estimate above ground carbon stock in the study area. The model was validated using independent data sets.

On average 70% of segmentation accuracy was achieved thus segmented CPA showed reasonable significant relationship with DBH (R^2 =0.79) and height (R^2=0.68). The coefficient of determination of CPA-carbon, DBH-carbon and height-carbon was 0.80, 0.92 and 0.74 respectively. Multiple regression model was developed using height from TLS and CPA from very high resolution image to estimate above ground carbon stock of plots and asses the inclusion of height from TLS to improved carbon estimates. The validated multiple regression model was relatively accurate (R^2=0.87) than the non-linear model developed using CPA only (R^2=0.84). However, above ground carbon stock of the study area was estimated from CPA only (non-linear model) since height from terrestrial laser scanner of the whole area cannot be detected from TLS. The amount of estimated carbon stock in the study area was approximately 185 Mg ha^{-1}. Even though the developed model was subjected to errors, it explained about 84% of observed carbon stock. Therefore, estimating carbon stock using data from TLS and very high resolution imagery in tropical rain forest is feasible.

Keywords: Segmentation, Object Base Image Analysis, Terrestrial Laser Scanner, Point cloud data, Regression, Allomertic equation, above ground biomass, above ground carbon.

ACKNOWLEDGEMENTS

First and for most I would like to thank the almighty God who helped me to accomplish this MSc. work with his power and love. He encouraged and helped me without limit in all ups and downs to reach at this level of success and I glorify his name.

I would like to take this opportunity to thank the Netherlands Government and the Netherlands organization for international cooperation in higher education (NUFFIC) for granting me a scholarship to study in the Netherlands.

My sincere gratitude and appreciation goes to my first supervisor Dr. Yousif Hussin for his valuable guidance, constructive feedback and comment from the very beginning till the completion of this study. I would like to thank my second supervisor Dr. Michael Weir for his valuable advice, feedback and continuous support during my study.

I am also happy to express my great appreciation to the entire staff of Faculty of Geo-Information Science and Earth observation (ITC) from whom I had a privilege of acquiring sustainable knowledge and experience during my study period.

I would like to acknowledge and express my thanks and appreciations for The University Technology Malaysia (UTM), Razak School of Engineering and Advanced Technology for their help and support to this research work. UTM supported me with housing, technical and instrumental support, transportation and data collection. My special thanks and appreciations to Dr. Khamarrul Azhari Razak for his excellent management and organization of the fieldwork campaign in Royal Belum expedition. Dr. Razak and UTM are highly appreciated for their generosity in every aspect of the fieldwork campaign. I am indebted to thank all team members who join the fieldwork in Royal Belum, Perak, Malaysia especially Dr. Kian Pang Tan of UTM Johor Bahru, Malaysia.

To my NRM and GEM students batch 2013–2015, many thanks for the unforgettable time we had together and thank you a lot for being a part of you guys.

I would like to acknowledge Miss Anahita Khosravipour, a Phd candidate in ITC for her kind technical support which helped me in my thesis.

My most hearted thank goes to my friend from Eritrea, Mr. Semere Tesfai Abraham for his support, encouragement and hospitability he showed during my ITC life. I will never forget you and may God bless you abundantly.

Last but not least, my everlasting gratitude goes to my family for their endless love, especially to my brother Mr. Meheretab Tquabo Sium and his wife Mrs. Adiam for their continuous encouragement throughout my study. God bless my family more.

Mebrat Tikabo Sium
Enschede, The Netherlands
February 2015

TABLE OF CONTENTS

LIST OF FIGURES

LIST OF EQUATIONS

LIST OF APPENDIXES

LIST OF TABLES

1. INTRODUCTION

1.1. Bakground

Forests are among the most important resources and provide many benefits. They sustain millions of animals that live in the forest and also provide social and economic benefits to communities who directly or indirectly rely on the forest. Most significantly forests cover one third of terrestrial ecosystem and play an important role in sequestration of CO_2 (Litton et al., 2003) and other greenhouse gases, thus stabilize climate/weather (Butler, 2012). Nevertheless we are losing the earth's forest at an alarming rate.

Deforestation and degradation of tropical forests is one of the main global agenda in forestry sector. Even though efforts on combating deforestation and degradation of tropical forests have been made, there are still indicators of degradation and deforestation in tropical forests and its effect on global carbon cycle (FAO, 2010). Several studies (Asner, 2009; Schwartzman, 2005) estimated 10-25% of global carbon emission from deforestation and degradation of tropical forests. Hence carbon of forests is decreasing (Gibbs et al., 2007; FAO, 2010) mostly associated with anthropogenic activities (Wright, 2005; Hamzah, 2012 ; IPCC, 2007).

In 1992 the United Nation Frame Work Convention on Climate Change (UNFCCC) established a framework to reduce greenhouse gases. Five years later the United Nation (UN) adopted the Kyoto protocol by setting legally binding requirements for emission reduction (UNFCCC, 1998). Accordingly all countries committed to UNFCCC and Kyoto protocol are required to report their national inventory to emission by sources and removal by sink on a regular base using effective methods (Gupta et al., 2003). Under the UNFCCC, an important agreement was reached in Bali in December 2007 encouraging developing countries to initiate actions to reduce emissions of carbon from deforestation and forest degradation (REDD) (Pelletier et al., 2012; Kanninen et al., 2010). REDD later expanded to REDD+ works on the main objective of mitigating climate change through reducing emissions from deforestation and forest degradation and removing greenhouse gases through enhancing forest management, hence conserve carbon stock.

As part of their incentives towards reducing CO_2 emissions as well as increasing their carbon stock, participating countries must be rewarded through carbon credits (Dulal et al., 2012 ; Gupta, 2012). On the other hand, industrialized countries are expected to pay for their emissions in the mechanism of REDD (Dhital, 2009). Hence countries must quantify and compare reduction of their CO_2 emissions using credible and verifiable scientific methods (Dhital, 2009). Accordingly each participating country must create a reference level, taking into account the circumstances and historical emissions trend. Therefore, REDD+ must carry out a reliable mechanism for measuring, reporting and verifying (MRV) changes in forest carbon stock on an annual base and countries must establish amendable MRV systems (Kanninen et al., 2010; Asner, 2011). Among REDD+ actions, most importantly, accurate measurement of 'change in forest area' and 'carbon stock density per unit area' are emphasized as the main variables to estimate change in carbon stock before offering carbon credit. Consequently the requirement for vigorous and accurate measuring and monitoring technique receive significant consideration (Pelletier et al., 2011; Calders et al., 2011). Then, it is contemporary concern to develop a scientific method that insures higher certainty of estimating carbon stock (Pelletier et al., 2011; Asner, 2011; Andrew et al., 2012). Based on this concern, this study aims to address the actual need to develop an accurate method of carbon stock estimates in tropical rain forest using data from very high resolution satellite imagery (hereafter referred to as VHRS) and Terrestrial Laser Scanning (hereafter referred to as TLS). In doing so, it is anticipated that the research will contribute in reducing uncertainties of governments and organizations employed on critical assessment of carbon stock changes, including REDD+ and its MRV system.

1.2. Problem statement

With the evolving of approaches for quantifying forest components, remote sensing offers stimulating possibilities because of its potential ability to cover large areas and its applicability to the estimation of above ground biomass (AGB) and above ground carbon stock in forest areas (Zheng et al., 2007; Lu, 2006; Mohren et al., 2012). Nevertheless, With complicated forest stand structure and diverse tree species composition estimation of above ground biomass remains a major challenge (Lu, 2005) especially in tropical and sub-tropical forests. According to Gibbs et al. (2007), the frequent saturation of remote sensing instruments' signal due to complex structure of the ecosystem is also one of the major challenges.
The direct measurements of harvesting and weighing to estimate total AGB and CO_2 flux have an advantage of being unbiased and precise, but are destructive and costly (Mohren et al., 2012). Rather, indirect methods using forest inventory data are cost-efficient, practical and provide reliable results (Mohren et al., 2012) as the data are collected at a required scales and from population of interest in a statistically well designed method (Brown, 2002). However, traditional methods are expensive and time consuming (Asner, 2009). For its applicability in extensive and inaccessible areas, remote sensing is a vital tool (Calders et al., 2011). Lu (2006); Gonzalez et al. (2010); Baker et al. (2010) highlighted the significance to associate remote sensing technique with carbon estimation methods that are calibrated by field measurement to quantify above ground biomass. For this instance several studies (Andrew et al., 2012; Baral, 2011) have been conducted to estimate AGB and carbon stock in forests. On the 17th conference of parties (COPs), UNFCCC also adopted the commitment that the national REDD+ measurement, reporting and verification (MRV) system shall be constructed on a combined field and remote sensing data (Vaglio, 2014).

Although the above techniques reduce cost of data and improves the quality of information (Baker et al., 2010), the main concern for implementing the articles of Kyoto Protocol is how precise the measurements are (Brown, 2002). Gonzalez et al. (2010) pointed out that greenhouse gas inventories and emissions reduction programs require scientifically robust method to quantify forest carbon storage over time across extensive landscapes. As it is a required to estimate carbon emissions with high certainty, a reliable methods for measuring, reporting, verification is essential (Köhl et al., 2009) for the countries playing a part in REDD+ mechanisms.

Among the parameters, diameter at breast height (DBH) is highly related to AGB and explains about 95% of variation in AGB (Brown, 2002). But diameter at breast height of tree cannot be detected from remotely sensed data. However there is a relationship between DBH and crown projection area (CPA) (Shimano, 1997; Hirata et al., 2009). CPA can be detected from very high resolution optical and Lidar sensor system providing opportunity to extract individual tree crowns through series of crown segmentation (Song et al., 2010; Gartner et al., 2008). Several studies (Hemery et al., 2005; Song et al., 2010; Lefsky et al., 2002) showed significant tree crown relations with DBH. In this context, measurements from optical images such as crown areas and ground based measurements can be applied to establish allometric relationships (Gibbs et al., 2007) for estimation of carbon stock with high certainty.

Tree height is essential supplementary parameter for carbon stock estimates. Lidar imagery directly provide height and canopy structure (Song et al., 2010; Lefsky et al., 2002) which can be used to estimate AGB integrating with data from optical images and field measurements (Karna, 2012; Maharjan, 2012). Since biomass is a function of volume, it can be derived from height. Meanwhile relationship exists between

DBH and CPA (Hirata et al., 2009), thus it is feasible that CPA and height will provide improved estimates of carbon stock.

The significant advancement in technology made automatic extraction of forest parameters such as DBH from TLS possible hence, its applicability in forestry seems to be practical at this time. The potential speed of data collection available in TLS techniques is desirable (Hopkinson et al., 2004) and demonstrated its potential and accurate estimation of AGB at plot level in eucalyptus species of Australia (Calders et al., 2013) even though it requires integrated approach and tools to extract meaningful information (Haala et al., 2004; Dassot et al., 2011). Likewise McHale (2008) underlined the application of TLS for forest measurements and cost effective, accurate ability of carbon stock estimates. It is now at the forefront as scientist begin to realize that the system is further accurate while measuring forest parameters since it avoids subjective readings from manual measurements and errors from variation in measuring devices (Simonse et al., 2003; Haala et al., 2004; Maas et al., 2008; Moorthy et al., 2008). Nguyet (2012) highlighted 2.1 and 4.5 kg errors in carbon estimation for "*Shorea*" and "other species" respectively could be from field base measurement. Similarly Chave et al. (2004) pointed out that 16% of uncertainty in AGB estimation is from measurements. In times where exact measurements of forest parameters are needed, TLS derived parameters are worthwhile to achieve desired certainty.

The Intergovernmental Panel on Climate Change (IPCC) guidelines categorize three methodological tiers based on the complexity to be used on national circumstances certainties. "Tier 1" uses globally available coarse data and involves large uncertainties and several assumptions. A more accurate method is "Tire 2" which uses more disaggregated data at the level of region or country with comparatively reduced uncertainties. Whereas "Tire 3" is a higher order approach which requires high resolution data and involves modelling and inventory of measurements with lower uncertainties as compare to Tire 1 and Tire 2.

Object base image analysis made extraction of tree crown by partitioning remotely sensed optical imagery with definite spatial and spectral scale. In this context integrating information from optical images with parameters from TLS is not yet fully discovered. Besides the previous studies with TLS were mostly done in temperate forests yet limited studies are done in tropical rainforests. Furthermore, achieving improved accuracy in methods with innovative remote sensing approach is necessary (Calders et al., 2011).

Thus this study will be aiming to explore the possibility of developing a method for accurate estimations of AGB with extrapolated forest parameters of DBH and height from TLS and CPA from very high resolution optical satellite image using object base image analysis in tropical rain forest of Royal Belum State Park, Malaysia. Considering the IPCC guidelines of "Tier 3", which requires development of accurate method at country level (Gibbs et al., 2007; Köhl et al., 2009) and fundamental challenges of MRV system, this research will have a viable contribution in developing an accurate method to estimate above ground carbon stock.

1.3. Research Objectives

General objective

The main aim of this research is to develop a method for assessing the relationship between DBH, height derived from Terrestrial Laser scanner (TLS) and Crown Projection Area (CPA) from very high resolution satellite imagery (VHRS) for estimating above ground carbon stock in tropical rainforest of Royal Belum State Park, Malaysia.

Specific objectives

1. To assess the relationship between segmented crown projection areas (CPA) derived from VHRS image and TLS derived DBH and height.
2. To assess the relationship between DBH and height derived from TLS and manually field measured DBH and height.
3. To assess the relationship DBH and height estimated from CPA and measured from field.
4. To assess the relationship of CPA from High resolution image, DBH, height from TLS and calculated carbon.

5. Research questions

1. How accurately CPA can be segmented from VHRS image?
2. Is there a significant difference between DBH and height extracted from TLS and manually measured from field?
3. Is there a significant difference between DBH and height estimated from CPA and manually measured from field?
4. Is there a significant relationship between DBH and height extracted from TLS and CPA segmented from VHRS images?

Research hypothesis

1. H_0: The accuracy of CPA segmented from VHRS is < 70%.
H_a: CPA can be accurately (≥70%) segmented from VHRS images.

2. H_0: At 95% confidence level, there is significant difference between DBH and height derived from TLS and manually from field.

H_a: At 95% confidence level, there is no significant difference between DBH and height measured from TLS and manually from field.

3. H_0: At 95% confidence level, there is no significant difference between DBH and height estimated from CPA and measured from field.

H_a: At 95% confidence level, there is significant difference between DBH and height estimated from CPA and measured from field.

4. H_0: At 95% confidence level, there is no significant relationship between CPA (from VHRS) and DBH, height (from TLS).
Ha: At 95% confidence level, there is significant relationship between CPA (from VHRS) and DBH, Height (from TLS).

1.4. Theoretical Frame Work of the Research

After reviewing relevant literature, the research problem was identified. Based on this identified problem, the research objectives and research questions were outlined. Then secondary data was requested and the required fieldwork was carried out to collect ground truth data and scan target objects. The collected data were analysed and the research discussed and concluded based on the results. The general description of the process is presented in Figure: 1 (Theoretical frame work of the research).

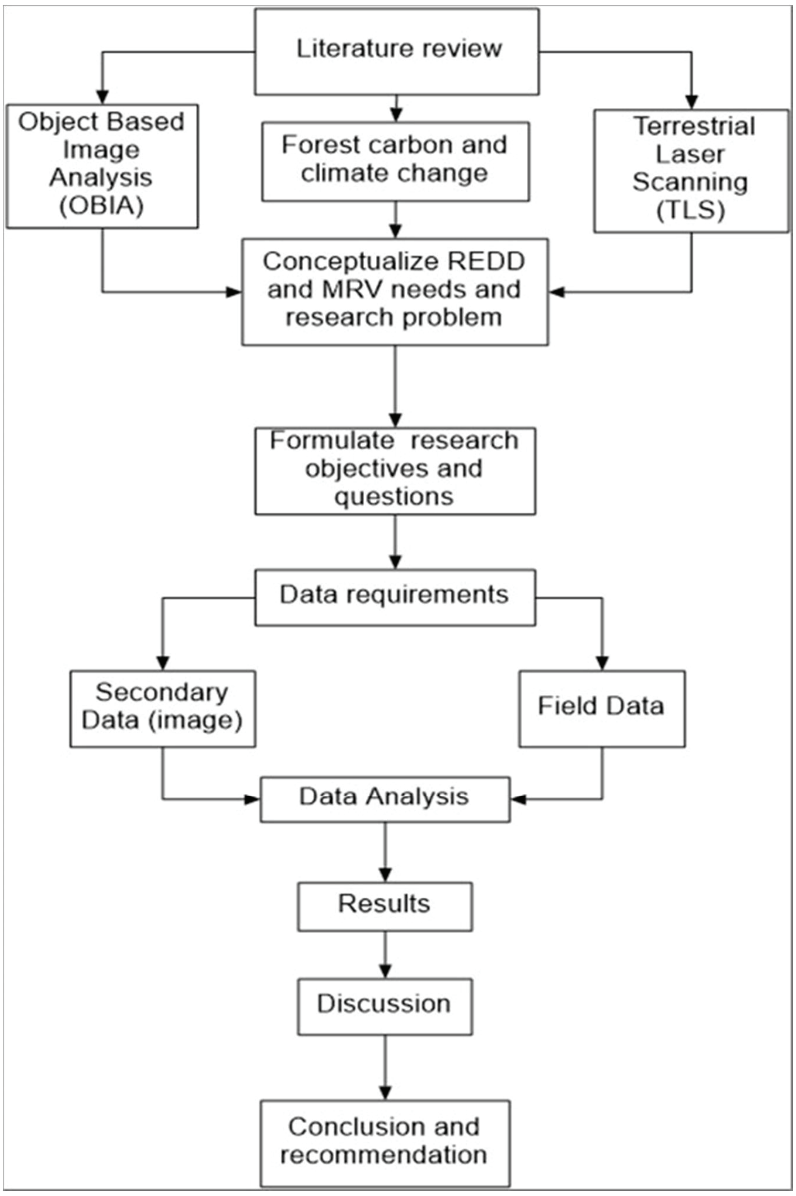

Figure 1: Theoretical framework of the research

2. LITERATURE REVIEW

2.1. Concepts and Definitions

2.1.1. Biomass and Carbon

Biomass is the total organic matter of dead or live weight per unit area of a plant (Antonio et al., 2009). It is a function of wood volume, wood density and architecture of a tree (Simone et al., 2008). Considering the ground surface as a boundary (Gschwantner et al., 2009), above ground biomass refers to the dead or living biomass of tree above soil including branches, leaves, stem, bark, foliage and seeds (Figure 2). While below ground biomass is the total biomass of live roots (Ravindranath, 2008). In this study the term "above ground biomass (AGB)" will be used to the total living biomass of trees above the ground surface. Estimates of dry weight biomass of trees and tree components are of interest to researchers (Jenkins et al., 2004; Brown, 1997) because above ground biomass stores most of carbon stock and are greatly affected by deforestation and forest degradation (Gibbs et al., 2007) moreover, it is an important sign of forest efficiency. Carbon is approximately 50% of oven dry biomass (Brown, 1997; Drake et al., 2002) or 47% (IPCC, 2007). Using this conversion factor, above ground carbon stock (hereafter referred to as carbon) of forests can be estimated from AGB. Even though it remains difficult to quantify, forest biomass is valuable measure in evaluating structural and functional attributes of forests efficiency.

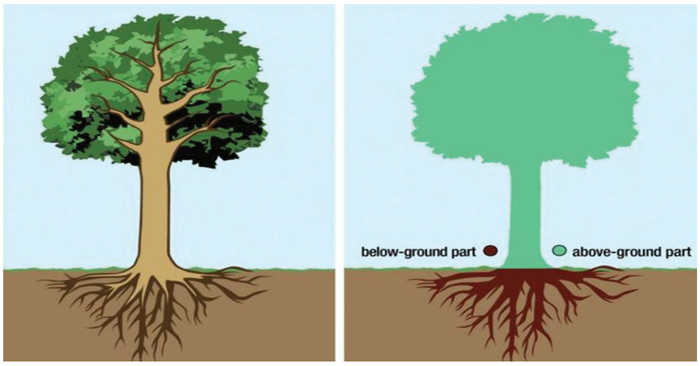

Figure 2: Above ground and below ground biomass

2.1.2. Allometric Equation

Allometric equations are most reliable method of estimating forest biomass without any destructive approach on the bases of established relationships between easily measurable dimensions of tree such as DBH (Simone et al., 2008; Ketterings et al., 2001; Wang, 2006). Choosing allometric equation is an important step in estimating AGB (Ekoungoulou et al., 2014; Chave et al., 2005). In tropical forests, where an area of 1ha may comprise more than 300 different tree species, it is very difficult to use species specific regression models (Chave et al., 2005). Moreover, developing allometric equations requires destructive sampling and may not represent the whole forest. Therefore grouping all species to use common and generalized equations is acceptable approach (Gibbs et al., 2007; Shah, 2011; Chave et al., 2005). The allometric equation developed by Chave et al. (2005) is suitable for areas with annual rainfall between 2250 – 3500 mm and covered with hard wood and tropical forests.

2.1.3. Crown projection Area

Crown projection area (CPA), also referred to as canopy cover, is the proportion of area on the ground covered by the vertical projection of the canopy (Jennings et al., 1999)(Figure 3). CPA is significant part of forest inventory however, it remains difficult to determine theoretically and practically (Rote, 2003). This is because it introduce error while measuring it for example: attempting to save time in field introduce errors (Korhonen et al., 2006). In addition to this Korhonen et al. (2006) mentioned deciding to include the gaps inside tree crown as part of the canopy or not makes it subjective and difficult to be accurate.

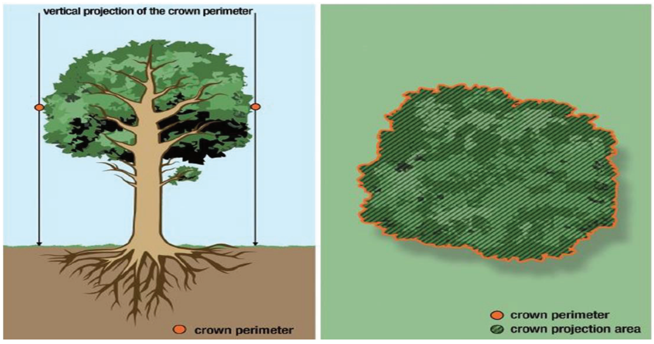

Figure 3: Demonstration of crown projection area (Gschwantner et al., 2009)

2.1.4. Object Base Image Analysis

With the increasing applications of high spatial resolution images and an alternative to poorly suited traditional pixel based classification; object Base Image Analysis (OBIA) is getting more acceptances. OBIA creates image-object thorough aggregation of pixels to image segments (Dragut et al., 2010). OBIA considers geometry and structure information in addition to spectral character to segment desired object of interest (Wei et al., 2005). In addition to this, humans can visually inspect to group similar toned and spatially arranged pixels (Hay et al., 2003). The software eCognition provides all the application tools of OBIA to extract information from high resolution imagery (Wei et al., 2005). The process of OBIA segmentation includes two major steps. First is to segment the image in to homogenous group of pixels to create image-object. The second step is to classify these image-objects based on colour, texture, shape and spectral information (Maxwell, 2006).

2.2. Principles of TLS

Terrestrial laser scanning is a light detection and ranging (Lidar) system that allow a non-destructive, fast and accurate acquisition of 3-dimentional (3-D) data with fixed x, y, z position and intensity value from the reflected signals (Dassot et al., 2011). The operating system of TLS technology is based on the emission-reception of laser energy which determine distance in two alternative methods (Rosell et al., 2009) namely: 1) by determining the time difference between emitted laser pulse from the sensor and reflected from the object back to the sensor and dividing this by 2 (time-of-flight Lidar) or 2) by measuring the phase shift between the incident and reflected laser beams (phase-shift measurement Lidar). In case of time-of-flight, the emitted laser deflects by a mirror to automatically scan the scene of the laser being reflected by the object. Then the complete hemispherical rotation of the device and scanning of a vertical plane by the deflected laser provides a comprehensive representation of objects in 3-D point cloud (Dassot et al,. 2011). In phase-shift measurement the laser scanner modulate the emitted light in to multiple phases and compares the phase shift of returned light then use an algorithm to fix the distance. Furthermore, Dubayah

& Drake (2000); Hall et al. (2005) have classified Lidar data based on foot print size and way of recording returned signals (Discrete and full waveform)

Discrete system records either one (single) return or few (multiple) returns for each pulse. These Lidar systems emits a small beam of light (0.2- 0.9 m in diameter) (Lim et al, 2003) i.e. small foot print, thus contains partial information of forest elements such as under estimation of canopy height in dense forests (Means et al., 1999). On the other hand, full waveform system record entire energy returned to the sensor for a series of equal time interval (Lim et al., 2003; Lefsky et al., 2002). They are categorized as wide beam light (8-70m in diameter) which permits large foot print area with various forest information (Means et al., 1999). These signals have equal importance in estimating variables (Lefsky et al., 2002). Most lasers for terrestrial applications generally have wavelengths in the range of 900-1064nm; where vegetation reflection is high (Lefsky et al., 2002; Hall et al., 2005).

The three dimensional coordinates (x, y, z) of target object are figured from the difference between laser pulse, the angle at which the pulse was fired and the absolute location of the sensor from the surface. Spatial registration of scanned data occurs during data acquisition because the location and orientation of sensor is known (Watt & Donoghue, 2005). Most scanners offer panoramic 360^0 horizontal field of view and vertical opening angle between 80^0 and 135^0 that allow hemispherical scanning (Bienert et al., 2006; Maas et al., 2008). Few scanners are also with a camera-like limited field of view (Bienert et al., 2006).

Figure 4: Sample of Terrestrial Laser Scanners

This study was carried out with RIEGL VZ-400 terrestrial laser scanner. RIEGL VZ-400 is a V-line three dimensional terrestrial scanner that offers high speed data acquisition by means of a narrow laser beam and a fast scanning mechanism. The high accuracy laser ranging is based on RIEGL'S sole echo digitalization and online waveform processing, which permits superior measurement. It is based on linear scanning mechanism through the rotating multi-sided mirror. It has GPS receiver integrated with antenna, internal data storage capability and various interfaces (LAN, WLAN, USB) (Riegl, 2013). The detailed specification of RIEGL VZ-400 is in Table 1.

Table 1: Specifications of RIEGL VZ-400 Scanner (Riegl, 2013)

Sensor	specifications
Field of view	100 X 360 degrees
Pulse rate	up to 122,000Hz
Range	up to 600 m
Accuracy	5mm
Beam divergence	0.3 mrad
Spot size	3cm at 100m distance
Minimum range	1.5m
Laser wavelength	Near infrared (1550 nm)
Camera	High precision digital NIKON D610

2.3. Overview and Techniques of Above Ground Biomass Estimation

Understanding forest biomass is important for several reasons. First, it provide an information about condition and productivity of forests (MacKay et al., 2011). Second, estimation of biomass is a means to obtain amount of carbon sequestered in forests (Ketterings et al., 2001). Also it is one of the facts to explain global carbon balance as an effect of deforestation (Ketterings et al., 2001). Several methods, techniques and tools have been used to estimate AGB/carbon stock. As the Intergovernmental Panel for Climate Change (IPCC) most importantly emphasized, accurate method of carbon accounting is prerequisite in monitoring carbon lose due to deforestation, forest degradation as well as gain from reforestation.

Lu (2006) examined three different approaches of biomass estimation. These were based on field measurements; remote sensing and GIS based methods. Field based measurement is the most accurate method since it directly harvests the forest and weighs the dry matter to estimate biomass. However it is destructive, time consuming and difficult to apply over large area (Asner, 2009; Lu, 2006). GIS based methods use data from existing limited inventory to generalize biomass estimation over large area (Brown & Gaston, 1995). However, getting quality ancillary data is difficult hence GIS based methods are not widely applicable (Lu, 2006). Remote sensing based methods are becoming widely applicable as extensive areas can be covered with reduced cost and efforts. Obtaining direct estimates of above ground biomass is difficult (Gibbs et al., 2007) and so this method establishes statistical relationship between remotely sensed and field measured tree parameters.

Remote sensing data and techniques have been extensively studied, using optical sensors (Lu, 2005), Synthetic aperture radar (SAR) data (Hajnsek et al., 2009) and also Lidar data (Lefsky et al., 2002). Synthetic aperture radar (SAR) employ an active sensors operating in longer microwave ranging from 1cm-150 cm (Waring et al., 1995). SAR technology has the ability to distinguish standing biomass estimates using single L-band cross polarized (HV or VH) irrespective of whether condition. SAR system sent signals that penetrate tree canopy have multiple scatter with in the tree canopy which then returns to the radar antenna. From these reflected signals it is possible to estimate tree parameters such as height (Gibbs et al., 2007). However, L-band (the longer wavelength available) tends to saturate at low biomass levels (approximately 150 Mg/ha), which makes SAR application limited (Waring et al., 1995).

Passive optical remote sensing systems data are available at low cost and used in most of remote sensing researches to estimate forest biophysical parameters such as biomass. The difference in sensors spatial resolution influences their range of application. Very high resolution (<5m) optical images are relevant for more specialized measurements of forest variables (Andersson et al., 2008) as well as essential means to extract visual information. Medium to low resolution optical images (>100m) are suitable for coarse scale mapping and multi spectral classification with limited classes (Gartner et al., 2008). Medium resolution satellite images such as Landsat are applicable in various fields including biomass estimations with improved accuracy at well aggregated grid-level (Lu, 2006). Unlike the medium resolution images, high resolution satellite images such as WorldView, GeoEye, QuickBird and IKONOS all with high spectral and spatial resolution, can detect physical dimensions of trees e.g. crown projected area (CPA) with high correlation to biomass (Gonzalez et al., 2010). However, very high resolution satellite images are least effective for pixel based image classification as spectral value among pixels greatly varies and result data redundancy (Wei et al., 2005). An alternative approach is object base image analysis, which gives a way to achieve desirable precision (Benz et al., 2004; Wei et al., 2005). In addition optical images are restricted by cloud cover and tend to saturate in dense tropical forests. Optical images also lack useful vertical information (height) that can improve the estimation of AGB/carbon stock (Hall et al., 2005; Hunter et al., 2013).

The recently emerging Light detection and ranging (Lidar) is an alternate remote sensing sensor system. Unlike optical sensors, Lidar technology extends the spatial analysis to the third (z) dimension and directly provides 3-D estimates of tree parameters such as height, canopy cover (Lefsky et al., 2002) hence gives biomass estimates with improved accuracy.

2.4. Works Related to The Study

Forest inventory for management and planning purpose requires measurements of tree parameters. Of these, the most important parameters are DBH and tree height (Maas et al., 2008). As large area forest inventory is not realistic by means of conventional techniques, inventory of isolated plots and statistical inference is the preferred method. Since estimation of carbon stock stored in forests provide an important figure on impacts of global changes (Brown, 1997), researches (Bryan et al., 2010; Asner, 2009) have been conducted to estimate above ground biomass from forest inventory and remote sensing.

Appling Object base image analysis with the use of very high resolution satellite images is an opportunity to help identifying individual tree crown (Gougeon & Leckie, 2006) and consequently estimating AGB. The study by Erikson (2004) with aerial image; Katoh et al. (2008) with airborne data and Tsendbazar (2011) with Geo-Eye image applied object base image analysis to delineate individual tree crown and achieved reasonable results. However, the complex nature of tropical rainforest with multi-layers of canopy affects accuracy of segmentation.

Although airborne Lidar has the advantage of wide area coverage, the precision and validity of technique depends on model's assumptions used to retrieve parameters from point cloud (Maas et al., 2008) and provide limited information under the canopy (Dassot et al., 2011). As an alternative for airborne Lidar and conventional remote sensing methods, TLS with the capacity of data processing technique with great detail and potential to reduce error is becoming a useful tool for forest inventory.

Watt & Donoghue (2005) in conifer forest and Hopkinson et al. (2004) in mixed deciduous plantations and red pine forest worked on extracting tree parameters from TLS data. Accordingly accurate measurements of forest variable such as DBH and height can be achieved though they recommend height could be a slightly underestimated from compact branching. Moreover Watt & Donoghue (2005) proposed future application of TLS for estimation of AGB. Hence McHale (2008) used DBH, height and tree density measurements from TLS together with allometric equations to predict carbon in Fort Collins Colorado, USA. Maan et al. (2014) assessed the potential of TLS for measurement of tree height and DBH to compute AGB in comparison to field data in sparse plantation and came up with reasonable coefficient of determination i.e. 0.79 and 0.96 for tree height and DBH respectively. Haala et al. (2004) investigated an inventory to collect forest parameters and identify tree species by integrating TLS and high resolution panoramic camera and demonstrated its applicability.

3. STUDY AREA, MATERIALS AND METHODS

3.1. Study Area

3.1.1. Criteria for Study Area Selection

Ease of access was one of the main reasons for the selection of the study area since the study has to be conducted with in limited time and budget. In addition to that WorldView-2 image of the study area was available. In spite of its significance on carbon sequestration as a tropical rainforest and complex forest stand structure, the study area is one of the least studied sites.

3.1.2. Geographic Location and Overview

The study was conducted in Royal Belum State Park (RBSP), in the northern part of Belum-Temenger Forest Complex (BTFC) in the state of Parek, northern Peninsular Malaysia. It extends over an area of 117,500 ha surrounded by Thailand in the north, the state of Kalantan to the east, Sungai Gandong in the west and Temenger forest reserve in the south (Figure 5). The area is highly protected primary tropical rainforest with rich biodiversity of flora and fauna which makes it one of the significant ecotourism and scientific research site. Apart from this, unique culture of native people living in the area with beautiful landscapes and lush sceneries are signs of attraction. The state of Perak gazettes the forest as permanent reserve for research since 2007. The east-west highway and Temenger Lake in the southern border are some spectacular features which provide access to the area.

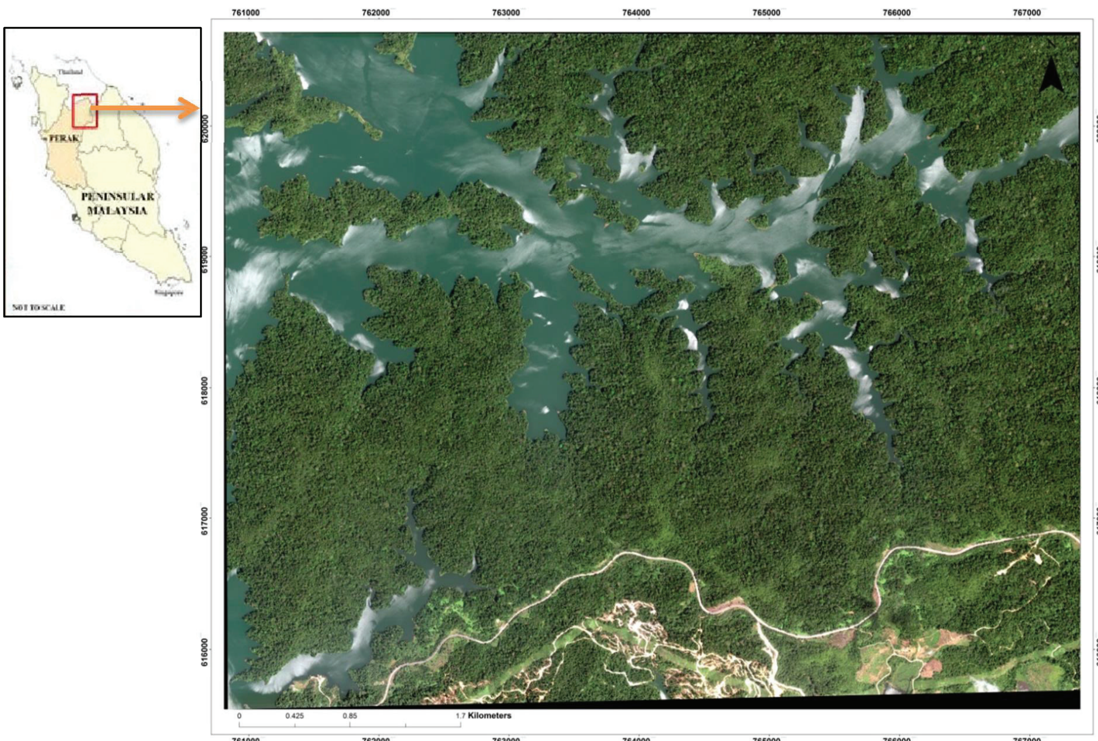

Figure 5: Location of the study area

3.1.3. Climate

The study area has a tropical monsoon climate with relatively high temperature (±24 ^{0}C - 29.9 ^{0}C) and high humidity ranging from 70 to 98% (Hanis et al., 2014). The annual rain fall of the area ranges between 2,160-2,250 mm. It receives highest rainfall in the wettest months of April and October. Whereas the area receives lower rain fall in the months of February and July (Hanis et al., 2014).

3.1.4. Vegetation

The tropical rainforest of the study area is recognized as one of the world's oldest rainforest (130 million years old). The forest type in the area are dominated by lowland *Dipterocarp,* hill *Dipterocarp,* upper *Dipterocarp* forest (Chye, 2010; WWF, 2014) extending from 260 m to 1,533 m above sea level. The majority of the species are characteristic of the tropical rainforest in peninsula Malaysia, Sumatra and Borneo, whereas the minority of the species is associated with seasonal tropical forest of Thai and Burmese type. The dominant plant species in the area are *Dipterocarpus costulatus* (Mersawa), *Shorea Platyclados* (Meranti bukit), *Intsia Palembanica* (Merbau).

3.1.5. Animal Species

The forest Royal Belum is well known for its habitat of globally threatened animal species. Some of the rare animal species in the forest includes Asian Elephant (*Elephas maximus*), Tigers (*Panthera tigris*), Sumatran Rhinoceros (*Dicerorhinus sumatrensis*) and all ten species of Hornbills found in Malaysia (Chye, 2010; Kaur et al., 2011). Besides around 316 species of birds have been identified in the forest including eight vulnerable species namely; Mountain Peacock pheasant *Polylectron inopinatum*, Wallace's Hawk Eagle *Spizaetus nanus*, Masked *Finfoot Heliopais Personata*, Large Green Pigeon *Treron Capellei*, Short-toed *Coucal Centropus rectunguis,* Blue-banded Kingfisher *Alcedo euryzona*, Plain-pouched Hornbill *Aceros subruficollis* and Straw-headed Bulbul *Pycnotus Zeylanicus*.

3.2. Materials

3.2.1. Data Used For the Study

3.2.1.1. Satellite Image

A very high resolution satellite image (VHRS) of WorldView-2 was used for this study. WorldView-2 is the first high resolution commercial satellite image with eight bands (Digital Globe, 2009). It has average revisit time of 1.1days with capability of collecting about one million km^2 of 8-band imagery per day (Digital Globe, 2009). WorldViwe-2 multispectral image comprises 8-bands of which four are in the visible electromagnetic spectrum namely, Blue, Green, Red and NIR_1 and four are new colours: coastal, yellow, red edge and NIR_2. For this study, only the first four bands were used. The image was acquired in February 2013 of both multispectral and panchromatic with 2m and 0.5m spatial resolution respectively. The image was geo-referenced to UTM WGS 84 coordinate system. The WorldView-2 image detail specifications are listed in Table 2.

Table 2: Satellite image specification (Digital Globe, 2009)

Specifications	WoldView-2
Spatial resolution	Multispectral: 2mx2m Panchromatic: 0.5mx0.5m
Band wavelength (μm)	Panchromatic: 450-800 Blue: 450-510, Green: 510-580, Red: 630-690, NIR_1:770-895
Acquisition Date	4/2/2013 4:17:05 AM
Sun Azimuth (degree)	91.50
Sun Elevation (degree)	74.80
Sensor Azimuth (degree)	323.50
Sensor elevation (degree)	64.90
Off-Nadir(degree)	22.30
Projection	Transverse Mercator
Coordinate system	WGS-84 UTM zone 47

3.2.1.2. Field Equipment

The equipment as listed in Table 3 was used for different data collection purposes during field-work. Navigation and recording coordinates of individual trees and plot centre was carried out with the help of GPS. Crown diameter in meters (m), plot diameter (m) was measured with measuring tape and DBH in centimetres (cm) was measured by diameter tape. Tree height was measured with Lieca DISTO D5 laser ranger in meters (m). Suunto compass, suuntu clinometer were used to measure bearing and slope respectively. Apart from measurements, TLS was used to scan trees in the plot as well as hemispherical camera to capture the canopy cover of the plots.

Table 3: Field equipment

SN	Type of instrument	Used for
1.	Terrestrial Laser Scanner(RIEGL VZ-400)	Scanning trees
2.	Diameter tape (5m)	Measuring diameter
3.	GPS	Navigation
4.	Measuring tape (30-50m)	Measuring diameter of plots
5.	Suunto compass	Measuring Bearing
5	Suunto clinometer	Measuring slope
6	DISTO D5 Laser ranger	Measuring height
7	Field work data sheet	Recording field data
8	Hemispherical camera	Capturing tree canopies
10	Densitometer	Measuring canopy density

3.2.1.3. Software

The research used several software depending on their purpose described in Table 4. Most of the statistical analysis was done in MS Excel, SPSS statistics22 and R studio software. While image analysis, GIS analysis and image segmentation was done in ERDAS IMAGINE 2014, ArcMap 10.2 and eCognition 9.0.2 respectively. The task related to writing and power point presentation was performed using Microsoft word and Micro soft Power-point 2010. TLS data was also analysed using RiSCANPRO software. The list of software used is presented in Table 4.

Table 4: Software used

Software	Used for
eCognition 9.0.2	Image segmentation
ArcMap 10.2	GIS analysis
ERDAS IMAGINE 2014	Image processing.
R Studio, SPSS statistics22 and MS Excel	Statistical analysis.
RiSCAN PRO 1.8.1	TLS data processing
Microsoft word 2010, Microsoft power point 2010	writing and presentation

3.3. Research Method

The method applied for this research can be described in three different processes. These processes are related to field data, remote sensing and statistical analysis. In the remote sensing related task: CPA, DBH and height were obtained from the image and TLS point cloud data respectively as independent variables of carbon stock estimation. Similarly DBH, height and crown diameter were measured from field as a ground truth. Finally a statistical analysis is carried out to analyse relationship between dependent and independent variables. The detail process and successive sections is shown in Figure 6, flowchart of the process.

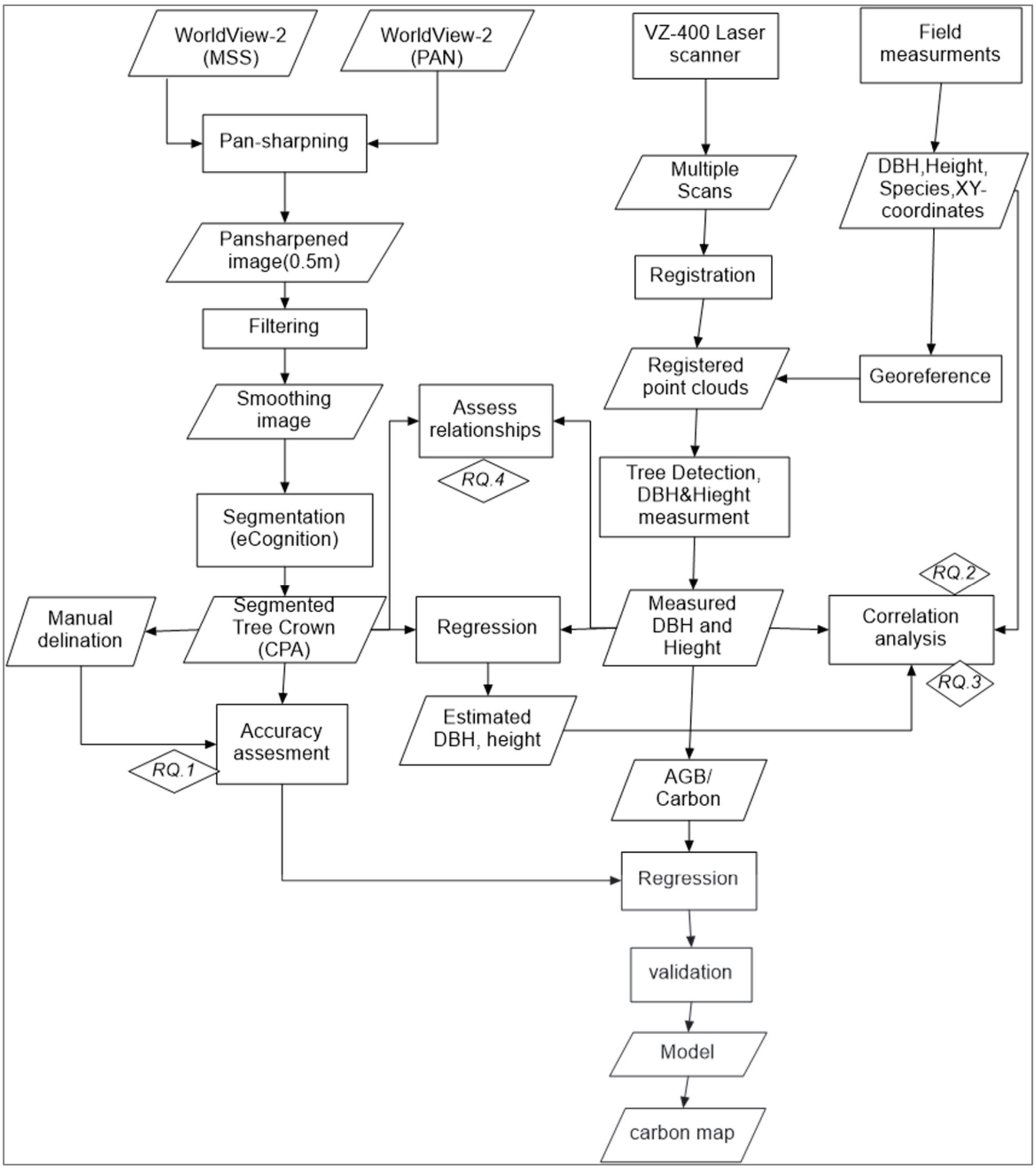

Figure 6: Flowchart of the process

3.3.1. Pre-Field Work

3.3.1.1. Sampling Design

The study applied purposive sampling strategy to represent all the trees in different forest canopy densities. Purposive sampling is non-probability sampling method used when sampling units are selected from a population to generate a sample with the intention to generalize. The tree canopies in less dense plots are more likely to be recognized from the satellite image than in dense plots with intermingled canopy. Besides the area south of the road (seen on Figure 5) have more open areas and less variation of species than the northern part. Since the ability to process point cloud data in very dense forest is challenging, the study considered to sample from less dense plots as well. Further, limited time, accessibility and topography of the area with the ability to work with TLS instrument were also taken into account while determining the plots. Therefore, the research used the mentioned strategy and collected 32 plots in which 6 plots were taken in the area south of the road (less dense) and the 26 in the northern part (dense) of the study area. Forest densities of the plots in the field were determined by Densitometer (an instrument used to measure canopy density) and visually with the help of high resolution image (WorldView-2).

3.3.1.2. Pan-Sharpening

Since satellite images provide data with different spatial, spectral and temporal resolutions, a full exploitation of these multisource data is required (Pohl & Genderen, 1998). Therefore, fusion/pan-sharpening technique is developed to provide improved information and reliable result from combined data (Pohl & Genderen, 1998).

Pan-sharpening is an image processing technique which aims to produce high-resolution multispectral images from fusion of multispectral low resolution pixels and panchromatic high resolution pixels (Padwick et al., 2010). Even though it is very difficult to obtain the original sharpness of panchromatic and colour of multispectral images, several fusion algorithms are practiced to get some quality information (Padwick et al., 2010). Among the various fusion techniques, Hue-Intensity-Saturation (HIS), Principal Components (PC) and High Pass Filter (HPF), Hyperspherical Colour Sharpening (HCS), Gram-Schmidt (GS) are some of the commonly used. In this study except GS these pan-sharpening techniques were tried with WorldView-2 multispectral of 2 m and panchromatic image of 0.5 m of spatial resolution to obtain the desired information. Hyperspherical Colour Sharpening (HCS) gave better impression visually than the others.

HCS is a pan-sharpening technique specifically developed for Worldview-2 imagery (Padwick et al., 2010). The technique processes any number of input bands with preserved balance between spatial and spectral quality. The technique involves mathematics which forward and reverse the transformations to and from the original colour space to hyperspherical colour space. Padwick et al. (2010) applied HCS pan-sharpening technique and quantified the performance of the algorithm on spatial and spectral quality of the resulting pan-sharpened image. The quality index measure by Padwick et al. (2010) found out that the technique is spatially robust as compare to PCA and GS and maintained reasonable colour balance. Pan-sharpening algorithm that preserves the spatial information of panchromatic image results better accuracy of image segmentation with OBIA analysis (Johnson et al., 2012).

3.3.1.3. Filtering

Filtering is a technique applied to remove noise associated with high resolution digital images. Low pass filtering smoothen an image by maintaining the low frequency and reducing high frequency information. A 5*5 low pass filtering/smoothing was applied in this study to enhance features and improved manual and automatic delineation of trees.

3.3.2. Field Data Collection

3.3.2.1. Biometric Data

Field work was conducted between September and October 2014. The objective of field work was to collect primary data which is required as ground truth from the actual study area. Circular plots with radius of 12.62m (500m^2 of area) were delineated. A circular plot is chosen for its advantage of least perimeter and easy to start at plot centre and walk out at approved distance in several directions to measure. Within each circular plot, tree height, DBH, crown diameter, tree species, x and y-coordinates of individual trees and coordinate of plot centre were measured with their relevant instruments and recorded in the data recording sheet (Appendix 5). Only those trees with DBH greater than 10 cm were measured since those with a DBH less than 10cm adds insignificant amount of biomass to the plot (Brown, 2002). Besides slope correction for the plots with more than 5% and aspect were also performed. All collected field data were compiled in excel file for further analysis. The main aim of collecting field DBH and height was for assessing the significance of correlation with DBH and height extracted from TLS.

3.3.2.2. Total Station

Total station is a surveying technique and equipment with integrated theodolite and electronic distance measurement (EDM) to define slope distance, horizontal and vertical angel of a specific point. From the total station, angles and distance of the plot centre were measured and x, y, z-coordinates relative to the location of total station was calculated. In this case at least two line of sight set in a points with known location are needed to determine the absolute location. Therefore, throughout the field work coordinate of two points were identified in straight line with the plot centre to calculate it's coordinate.

During scanning time a default coordinate is given to the point cloud data by the sensor. The calculated coordinate from the total station was used to geo-reference scanned data. Geo-referencing refers to the process of transforming coordinates of geographic features in to absolute reference system (Chekole, 2014). In this case the scanned point cloud data with 3-D coordinate of laser sensor frame are transformed in to mapping frame (Chekole, 2014). Coordinates measured by total station have high accuracy and precision (Chekole, 2014) thus this technique was used in this study. Measurement of total station of this study was done by the survey team of University Technology Malaysia (UTM). Figure 7 shows a sample reference map of one plot used by the team.

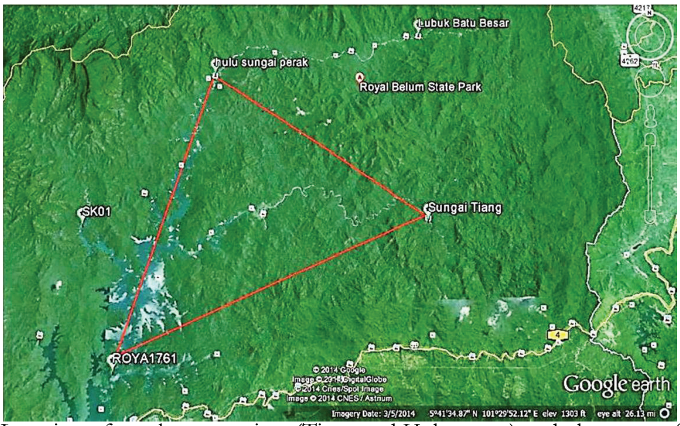

Figure 7: Location of two known points (Tiang and Hulu sunga) and plot centre (ROYA 1761)

3.3.2.3. TLS Data Acquisition

Before the actual scanning time, several procedures should be taken in to consideration to obtain quality scanned point cloud data. The main procedures taken in this study are in the following subsections.

Scan position setup

Acquiring point cloud data using TLS has two approaches: single and multiple scan (Olofsson et al., 2014) (Figure 8). Single scan approach uses only one scan from the centre of the plot and represents one side of trees in the plot. Whereas multiple scan approach scan from different positions of the plot and represent several views of the trees, later needs to be mended to a common coordinate system. To ensure reasonable overlap of scanned data, greater canopy height, improved quality of information and 3-D representation of objects, a multiple scan is required (Watt & Donoghue, 2005; Calders et al., 2014; Thies et al.,, 2004). Therefore this study followed the multiple scan approach. Scan positions were chosen depending on the overview of the forest structure inside the plot. For every plot four scan positions were ideal i.e. one at the plot centre and three other positions outside in more or less 120^0 apart from each other. The distance between plot centre and the three scan positions were determined depending on the topography i.e. preferably less steep. In this study these scan positions were fixed around 2-3 m away from the plot boundary to obtain maximum coverage of tree height and avoid blind spot. Even though it was difficult with topography of the area, further increase in distance of the scan position also maximize scan of unwanted areas.

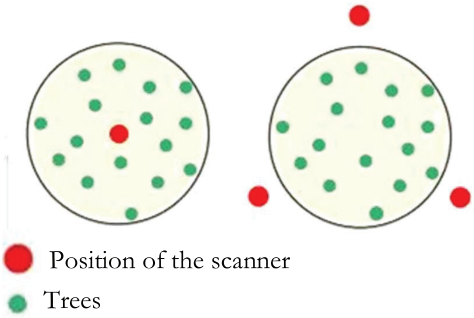

Figure 8: Demonstration of single and multiple scan positions using TLS

Setting Tie points (retro-reflective objects)

Tie points are highly reflective objects which are used as a reference points for co-registering multiple scans. This study was aimed to follow tie point based registration thus, considering the possibilities of misdetection by the sensor or occlusion by the trees, 15 tie points were fixed in each plot. The types of tie points used were both cylindrical 3-dimantional and circular 2-diamentional retro-reflectors. The 2-dimantional tie points were pinned in to the trees' stem around the central position of the canner whereas the cylindrical were kept on top of a standing stick with more than 1m height from the ground (Figure 9). In addition to this, the following considerations were taken into account as cylindrical tie points should be:

- Evenly distributed with nonlinear pattern
- Levelled with the tripod to avoid blocking by the undergrowth vegetation
- Within the range of scanner distance
- Visible to the scanner from all the scan positions
- Stable on their stand position

Figure 9: A sample of cylindrical tie point from the field.

Setting TLS and scanning

Data acquisition was carried out by a terrestrial laser scanner RIEGL-VZ-400 with a digital camera NIKON D610. The horizontal and vertical field of view of the scanner is 360^0 and 100^0 respectively. The rotating design and multi-sided mirror enable the instrument to acquire data on its maximum field of view.

In all cases the instrument was fixed on a tripod to scan from preferable position where it is levelled and possible to see most of the target trees. Levelling was done manually with the help of built-in levelling tool to align the instrument horizontally and vertically. Prior to scanning each scan was saved as a new project with specified scanner settings. In the main menu of scan position set up, the same scanner setting were used through all the scans as summarized in Table 5, except brightness of the image were modified in some dark plots. The reflectance threshold was set to 0.05 decibel (db). Reflectivity value allows easy estimation of target's reflectivity. Value above 0 db implies that the target gives an optical echo amplitude larger than those of a diffuse white target, i.e. the target is retro-reflecting which easily can be recognized (Riegl, 2009). During early actual scanning time, true colour photographs of the entire field of view were taken automatically with the integrated above mentioned camera. In this case minimum of seven pictures for each scan position in a plot were taken for visual interpretation of the data. Then the instrument scans the scene once where, the retro-reflective objects appear as red spots. At this stage the retro-reflective objects were searched manually using reflector search function. This function allows the system to write the coordinate of retro-reflective objects and list them as corresponding tie points. With listed reference of these retro-reflective objects, the whole scene was scanned again and saved as one scan position. The scan data was in range form with panaroma-60. Panaroma-60 was chosen since this scan provides a full 360^0 field of view with medium resolution. Since trees were the object of interest, panaroma-60 was reasonable resolution to identify individual trees. It also takes less time of scan than panaroma-40 of fine resolution. The immediate result of scanned scenes is point cloud with determined position (x, y, z) and intensity of the reflected signals (i). Figure 10-12: shows scenes of scanned data in different selection view type.

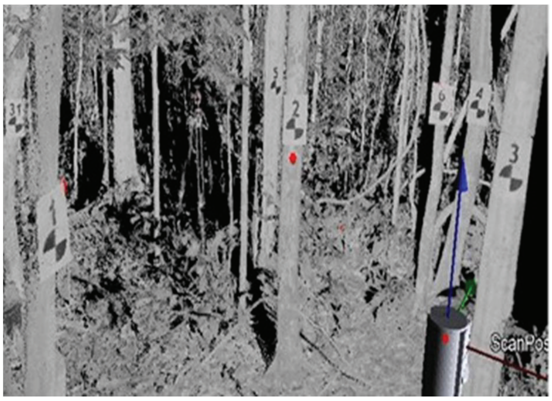

Figure 10: Scanned data in 3-D linear scale

Figure 11: Scanned data in 2-D intensity linear scale

Figure 12: 3-D Scanned data in true colour linear scale

Table 5: TLS settings during scanning

Sensor	settings
Image acquisition	Accurate
Reflector threshold	0.05db
Scan mode	Panaroma-60
Range	50m
Scan form	Range
Reflector size	>10cm

3.3.3. Field Data Analysis

3.3.3.1. Manual Delineation of Trees

Recognizing actual tree crown in tropical rain forest is a challenging task. Thus even though the number of trees measured in field were 698, only 279 (39.9%) were manually delineated in the image. Manual delineation of recognized trees on the image is mainly performed for assessing accuracy of automatic segmentation and model validation. Delineation of recognized trees was done in ArcGIS with 5*5 filtered pan sharpened multispectral image. The panchromatic image was also used to alternatively check in some cases while identifying tree crows. The suitable band combination was 4:3:2, same as used in eCognition software for automatic segmentation. With the overlaid shape file of sample plots, the recognized trees were delineated at the same scale of 1:250. Field measured crown diameter was used as reference to avoid over and under estimation of manual delineation.

3.3.4. Segmentation

Segmentation is a process of partitioning of a digital image into non-overlapping discrete regions or spatial clusters based on spectral, spatial and textural homogeneity (Ryherd & Woodcock, 1996). The process of segmentation minimizes the with-in class spectral heterogeneity of very high resolution images to simplify the representation of an image into image objects and extract meaningful information (Dragut et al., 2010).

Image objects with defined homogeneity, size and shape are the building blocks for further image operations (Definiens, 2008) and determine quality of segmentation, thus defining image object is an essential step of segmentation process (Kim et al., 2008). Basically there are two segmentation approaches namely: top-down and bottom-up approaches with several algorithms to refine image objects according to a given criteria (Definiens, 2008). Top-down approach starts with larger object or the entire image and partition in to smaller objects. Chessboard and quad-tree base segmentation are an example of top-down segmentation approach (Definiens, 2012).

Whereas bottom-up also known as region based approach creates large objects by assembling smaller ones or pixels (Definiens, 2012). In several successive steps, smaller image objects are fused in to larger ones. All through this pairwise merging process, the fundamental optimization technique results in subsequent image objects with minimum weighted heterogeneity. Multi-resolution segmentation is an example of region based segmentation technique (Definiens, 2012).

3.3.4.1. Multi-resolution Segmentation

Multi-resolution segmentation is one of the sophisticated and successful algorithms of region growing approach. Multi-resolution method starts to segment from one pixel and grows by merging the best fitting neighbouring pixels to create an image object with defined minimum heterogeneity (Benz et al., 2004). Through successive merging process the whole image segments in to a number of larger image objects/regions with minimum heterogeneity (Figure 13). A segmented object is defined as homogenous on the basis of its shape and spectral homogeneity (Definiens, 2012). The Pixel with exceeded threshold of local homogeneity value restricts the boundary of image objects/regions and become a new seed. This study used multi-resolution segmentation which was carried out in eCognition developer 9.0.2.

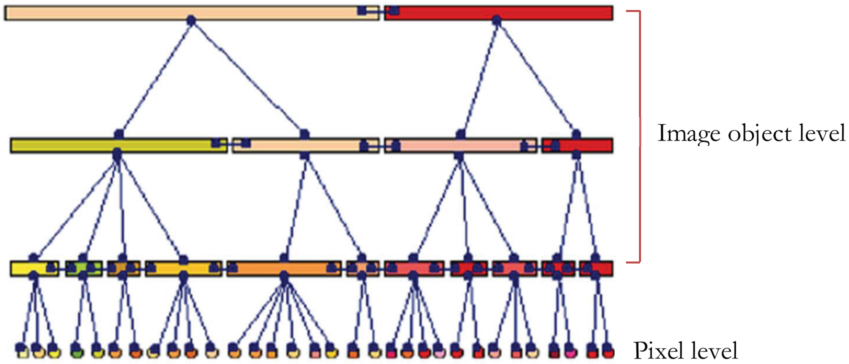

Figure13: Illustration of multi-resolution segmentation process (Benz et al., 2004)

3.3.4.2. Scale Parameter

Determining image objects' size using scale parameter in multi-resolution segmentation is a challenging task of segmentation. It is subjective measure that the user generate image objects that represent real world objects with determine scale parameter. Therefore, it requires a series of trial and error to get the optimum scale. Scale parameter is a threshold that controls degree of heterogeneity in segmented image objects. Heterogeneity and homogeneity of input data influence size of resulting image objects and the scale parameter at which the objects get well segmented. Larger scale parameter allows merging of more pixels and subsequently larger objects, and vice versa.

The criterion for homogeneity is combination of spectral components (colour) and shape (compactness and smoothness) all known as composition of homogeneity (Figure 14). The sum of these user defined weight parameters i.e. shape-colour and compactness-smoothness is 1. The value for shape determines the weight between shape and colour, similarly value for compactness determines the weight between compactness and smoothness (Kavzoglu & Yildiz, 2014).

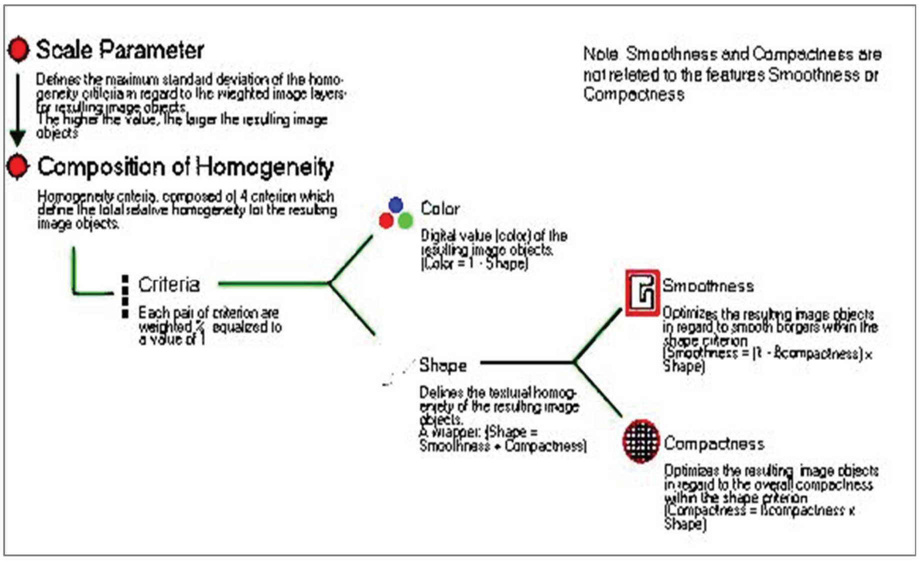

Figure 14: Multi-resolution concepts flow diagram (Definiens, 2012)

3.3.4.3. ESP Tool for Estimation of Scale Parameter

With increasing applicability of OBIA to extract meaningful information and its subject of identifying optimal scale parameter, ESP tool is developed as a technique to estimate appropriate scale parameter of image segmentation (Dragut et al., 2010). The tool works in bottom up approach and iteratively produces image objects and calculate rate of change of local variance (ROC-LV) at multiple scale levels. It plots ROC-LV against scale values where it shows peaks of multiple scales implying the suitable level at which the image can be segmented properly. Figure 15: shows the ESP tool for estimation of scale parameter.

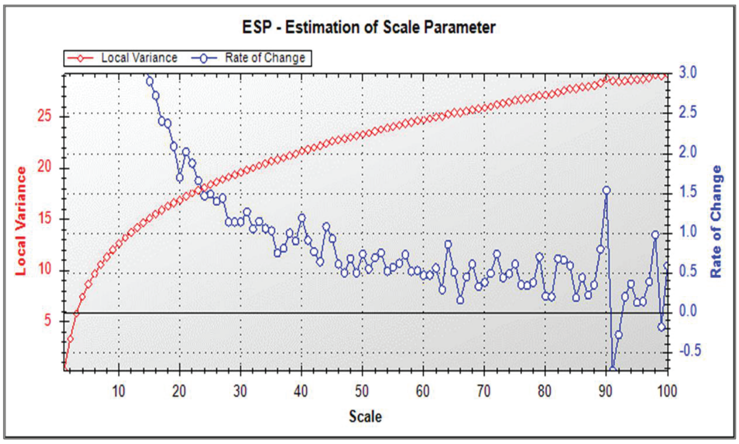

Figure 15: ESP tool for determining scale parameter (Definiens, 2012).

3.3.4.4. Masking Out of Shadow, Water Bodies and Bare Areas

Due to nature of high resolution images and viewing angle, shadow appear in most parts of the image. In the early phase of segmentation shadows were separated from trees and masked out using mean brightness value. An assumption is made that shadows have lower mean brightness than trees. A considerable part of the study area is covered by water bodies, bare areas and by the road in the southern part of the study area. Therefore, masking these non-vegetated parts of the image was needed as part of segmentation process. While developing a rule set, the reflectance value of the objects on different bands were checked. Among the image bands, near infrared was weighted as more important than the other bands so as to achieve maximum spectral information of trees.

In masking out the water bodies, mean reflectance value of near infrared band was preferred as trees have distinct reflectance value in this band. In this case pixels with high reflectance value in near infrared band were considered as trees and with lower reflectance (<50 in this study) of the same band were masked out as water body. On the other hand bare areas including the road were masked by updating the range in mean reflectance value of red band. Mean reflectance greater than 192 was a suitable value to mask out bare areas.

3.3.4.5. Watershed Transformation

In segmenting dense tropical forest with overlapping tree crowns, the watershed transformation algorithm is widely used to separate the intermingling tree crowns into individual tree crowns on the basis of splitting threshold. The splitting threshold is set on the basis of average tree crow width measured in the field and expert knowledge. The algorithm considers the image as an inverted topographic surface (Figure 16). In an inverted image, the distance of each pixel in an image object to its border becomes overturned distance. This means the local maxima in the original image becomes local minima in the inverted image (Definiens, 2012). The inverted image looks like watershed catchment where the local minima become punched holes and the local maxima a watershed lines. In between the local maxima and minima appears the watershed basins which are corresponding tree crown in the original image.

Once water is introduced in the system, each valley collects water from the local minima until water splits in to the neighbouring valley (Wang et al., 2004). Each valley is surrounded by watershed lines separating the whole area in to several catchment basins and creates suitable boundaries. Therefore, in time of applying watershed transformation to the forest, tree clumps are treated as the catchments and under flooding water assumption, the trees (valley) touch each other and then those trees are separated into individual trees.

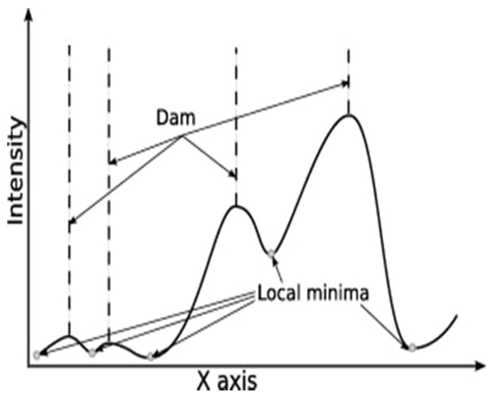

Figure 16: Illustration of watershed transformation (Beucher, 1992)

3.3.4.6. Morphology

Morphology is an operation used for smoothing image objects, in this case tree crown. The algorithm has two possibilities, namely open and close image objects. Open image object operation eliminates pixels which are isolated from an image objects to have more regular shape, whilst close image object add surrounding pixels to an image object to fill small gaps resulting from e.g. shadow effect. Furthermore the circular and square mask options in morphology are the base for structuring image objects. Since a tree crown is approximately circular, circular mask and close image object was applied to give the appropriate shape.

3.3.4.7. Removal of Undesirable Objects

After the above mentioned operations of segmentation procedure, removal of undesirable objects was performed. This process was aimed to eliminate smaller and elongated segments on the basis of area of pixels and roundness values to produce more smoothed tree crowns. In this study, tiny segments with pixel area of less than 16 were removed since they hardly can be detected as tree crowns. In addition to this, elongated segments which are unlikely to be tree crowns were removed.

3.3.5. Segmentation Validation

Validation of automatic image segmentation was carried out mainly to evaluate its degree of fitness relative to that of known objects. Validation of segmentation is related to quality of data (noise, spatial and spectral resolution) and optimal customizations of parameter settings (Möller et al., 2007) which determines matching of segmentation results on target objects. Accuracy assessment of segmentation can be achieved in different ways. However, it basically considers the topological and geometrical relationships of two matching objects (Möller et al., 2007). Topological relationships of objects consider their 'containment' and 'overlap' while; geometric relationships of objects is ascertained by the comparison of object positions.

The approach developed by Möller et al. (2007) assess accuracy of automatic segmentation based on relative area in reference to manually digitized polygons. In this way, a best score is given if the manually digitized reference polygons are fully enclosed by automatic segments. At least 50% overlap of reference and automatic segments is considered as acceptable (Zhan, 2005). Meanwhile matching of segments take size, shape and position into account as completeness and correctness (Zhan et al., 2005).

Variation in matching of segmented objects with their reference objects is demonstrated in Figure 17. The orange part of the polygon is matching well between automatic segment and its ground truth reference polygon; green part is the region in segmented object but not explained by its reference whereas blue part is a region in reference object but not explained by segmented object. In this case, (a) Indicates the match between reference polygon and automatic segment is more than 50%; (b) matching of both objects in size and shape but not location and in (c) and (d) the position of reference polygon and automatic segments matched but with variation in spatial extent (Zhan et al., 2005).

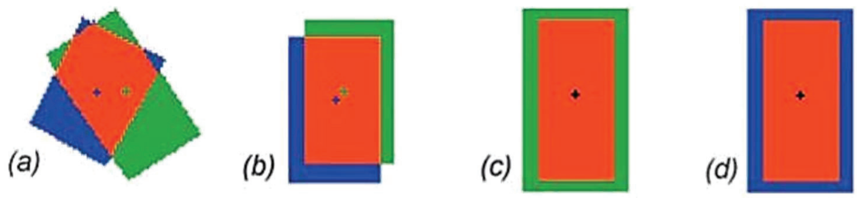

Figure 17: Variation in matching of polygons (Zhan et al., 2005)

On the other hand, the segmentation accuracy assessment developed by Clinton et al. (2010) basis on geometric extent of automatic segments with reference polygons and quantify the accuracy in terms of over and under segmentation. Over segmentation and under segmentation are explained by Clinton et al. (2010) as follows (Equation 1 and 2)

$$Over\ segmentation = 1 - \frac{area\,(xi \cap yj}{area\,(xi)}, yi \vdash Yi' \qquad \text{.....................Equation 1}$$

$$Under\ segmentation = 1 - \frac{area\,(xi \cap yj}{area\,(yi)}, yi \in Yi' \qquad \text{.....................Equation 2}$$

Where: xi is reference object and yj is its corresponding segmented object.

The value of segmentation is explained in terms of distance index (D), means 'goodness of fit' which is a combination of over and under segmentation. The D value of segmentation ranges from 0 to 1, where 0 indicates perfect match between reference and segmented objects and 1 is minimum mismatch. Goodness of fit of segmentation is calculated as in Equation 3.

$$D_{ij} = \sqrt{\frac{Oversegmentation_{ij}^2 + Undersegmentation_{ij}^2}{2}}$$ ……………………Equation 3

3.3.6. Point Cloud Data Analysis

Processing of point cloud data was done using RiSCANPRO software provided by RIEGL. RiSCANPRO is companion software for 3-D terrestrial laser scanner systems. The data acquired by the system is organized and stored in RiSCANPRO's project structure. The entire data includes scans, digital images, GPS data, coordinates of tie points and all transformation matrices used to transform the multiple scan in to well-defined common coordinate system. In addition to this, the software provides several functions for data processing. The details of the processing steps done in the study are presented in the sub-sections below.

3.3.6.1. Registration

Registration of point cloud data refers to the adjustment of scans by integrating local patterns into common reference (Chekole, 2014). The first scan was taken in the centre of the plot and was used as a common reference for overlapping the objects that exists in multiple scans of the same scene. Registration can be done in two ways (Bienert & Maas, 2008): marker free and marker based registration. Future based (marker free) registration method uses an extracted feature such as edges, planes or points as a base for registration while, Iterative Closest Point (ICP) apply an algorithm to iteratively register two overlapping cloud points on the basis of their minimum Euclidean distance. In case of marker based, reflective targets (tie points or markers) must be placed with in the plot for later to be recognized by the user as corresponding points of registration. In this case the identified tie points placed around central scan were used as common reference to match the multiple scan positions in this study.

In some cases multiple scans could intersect rather than merging around the stem resulting in smaller tree stem or may not meet well, hence leading in larger stem than the actual. As recommended by Hopkinson (2004), these effects can be reduced by using more tie points. Similarly the study by Bienert & Maas (2008) achieved best alignment of point cloud from multiple scans using nine tie points than four. This study followed marker based registration approach using 16 tie points in every plot and merged multiple scans to a common reference which is the scan taken from the centre. Marker based registration is precise (Bienert & Maas, 2008) however, placing tie points throughout the scanning area is time consuming.

RiSCANPRO program uses three different coordinate systems, i.e. Scanner's own Coordinates System (SOCS), Project Coordinate System (PRCS) and Global Coordinate System. SOCS is scanner's own local coordinate system (Cartesian x, y, z coordinates) delivered to the raw data. While PRCS is a user defined coordinate system such as coordinate system at the scan site. In case of GLCS, the coordinate system is embedded usually form externally recorded coordinates. During registration tie points were needed to convert the local coordinate system of multiple scans, (valid for one scan) to global coordinate system, (valid for all scans) (Seidel, 2011). Coordinate of minimum three tie points visible at least from two different scans were identified as corresponding points (control points) of linking the coordinate of multiple scans to the centre. This means, all the multiple scans are transformed to the coordinate system of central scan as a common reference with global coordinate system which is imported to the project system which is externally collected from total station.

3.3.6.2. Plot Extraction

The scanned point cloud data includes large areas that are not of interest. Thus trees with in circular plot of 12.62 m radius (500m^2) or more in some plots with higher slope (according to field records) were filtered since these were the target of the study. The points within the range of distance were selected using the range function in the selection mode of RiSCANPRO. This was mainly done to determine the area of interest and save processing time by excluding unwanted points.

3.3.6.3. Individual Tree Detection

Each measured tree in the plot was tagged with a number as unique identifier in the field. Identification of individual trees with in the point cloud was done manually. Here an assumption was taken that a tree stem appear as a distinct and enclosed circle of points (from the top view) (Hopkinson et al., 2004) which is distant from adjacent stem and continue several meters up. In this way an individual tree stem is identified from the proximate point clouds related to the ground and foliage. Unavoidable natural situations such as splitting tree stem and closeness of trees' stem were possible. Identification of individual tree was done in the reflectance linear scale of selection view.

3.3.6.4. Individual Tree Extraction

Selection of associated point clouds of an individual tree were performed in the viewer mode window of RiSCANPRO. The smallest crown diameter of tree measured from the field was used to set radius horizontally around the point cloud associated with individual tree. By visual inspection, debris, foliage, parts of neighbouring trees were removed in successive steps manually. In the higher part of the tree, spacing between points increase thus, in some cases separating point clouds of crown associated with target tree from neighbouring trees was difficult. Therefore, minimum horizontal distance along the dense enclosed circle of tree stem was taken on the upper part of the trees since crown size was not the target of the study. In this way recognized trees were sliced and saved as a polydata for measurements.

3.3.6.5. Tree Height Measurement

Every extracted single tree in the polydata was exported to ASCII file format. Then tree height was calculated as a difference of the highest and lowest point cloud in Z-value (Figure 18).

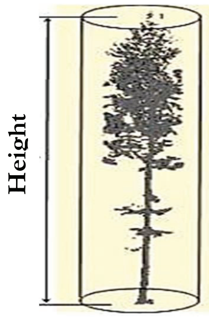

Figure 18: Determination of tree height (Bienert et al., 2006)

3.3.6.6. DBH Measurement

For every single tree diameter at breast height was determined at 1.30 m from the lowest identified point (Figure 19). Measurement of diameter at breast high was done manually using point to point measurement. In the viewer mode window of RiSCANPRO, the tree stem at 1.30 m is selected as different colour and zoomed in for enhanced visibility of points. The measurement tool reads every x, y, z value of the points and measurements were taken from point to point along the horizontal distance of the stem as DBH.

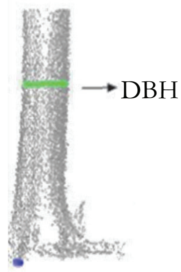

Figure 19: Determination of DBH. Modified from (Bienert et al., 2006)

3.3.6.7. Comparison of DBH Measured From Field and TLS

The correlation analysis of extracted height and DBH from TLS and measured from field was carried out. This was aimed to assess the significance of the relationship between these two measurements. The analysis of significance test was done using paired t-test and F-test in Microsoft Excel 2010.

3.3.7. AGB and Carbon Stock Calculation

Appling allometric equations is most common method of computing above ground biomass (Ketterings et al., 2001) since it allow estimation of vast forest areas without distraction of forests. Hence, carbon stock is calculated using the conversion factor that accounts 0.47 % (IPCC, 2007) of entire above ground dry biomass. Nevertheless choosing appropriate allometric equation requires careful consideration of their suitability. There are several allometric equations developed for estimation of biomass in tropical forests. Ketterings et al. (2001) and Basuki et al. (2009) developed local allometric equations in estimating above ground biomass of forests in Indonesia. However local or regional allometric equations showed lower performance as compare to generic models (Rutishauser et al., 2013). In tropical rainforest which comprise more than 300 species, species-wise allometric equations are not necessarily appropriate to generate reliable estimates of aboveground biomass (Gibbs et al., 2007). Appling generic allometric equations stratified by ecological zones increase precision of estimates since the equations tend to be established on a larger number of trees and include wider range of DBH (IPCC, 2007; Gibbs et al., 2007; Chave et al., 2005; Brown, 2002). The widely used generic equation developed by Chave et al. (2005) is recommended by IPCC guidelines in terms of REDD+ for estimating above ground biomass of moist tropical forests with around 2000 mm of rainfall. Thus the generic allometric equation developed by Chave et al. (2005) (equation 4) was used since the study area is located in a similar environment. The equation considered both height and DBH with wood density of trees which varies among species.

$$\mathrm{AGB} = 0.0509 \times \rho D^2 H \quad \text{...................................... Equation 4}$$

Where,
AGB: above ground biomass (kg);
ρ: Wood specific gravity (gcm^{-3});
D: diameter at breast height (DBH) (cm); and
H: tree height (m)

Using the conversion factor, the calculated AGB was converted to carbon stock (Equation 5).

$$C = B * CF \quad \text{...Equation 5}$$

Where,
C: carbon stock (MgC)
B: dry biomass
CF: carbon fraction of biomass (0.47)

3.3.8. Correlation Analysis

Prior to model development, correlation analysis of variables is an important and required in scientific research. Thus it was carried out for both data extracted from TLS and satellite image. To determine the relationship between variables, a scatter diagram was made. DBH and height from TLS were plotted against CPA extracted from image. Similarly the relationship of these variables and observed (calculated) carbon was illustrated. Coefficient of determination which indicates rate of variation in one variable as a result of change in another variable was computed. Regression analysis of response and explanatory variables was done. Based on that, a model was developed and validated. Paired t-test was used to analyse mean difference of DBH and height measured from TLS and manually from field. Similarly the established relationship between CPA and DBH, height from TLS was used to estimate DBH and height as possible approach to estimate carbon stock. The estimated DBH and height was compared with field measured DBH and height.

3.3.9. Regression Analysis and Validation of Model

Regression analysis was performed mainly to inspect the relationship of dependent and independent variables, determining an expected change in the independent variable as a result of change in the dependent variable (Husch et al., 2003). After visual investigation of data distribution with scatter plot and box plot, some outliers were removed as required to establish robust model prior to regression (Mora et al., 2010). Thus non-linear relationship was established between CPA and carbon to develop a regression model. In this case CPA segmented from image was considered as independent and calculated carbon as dependent. The total number of trees recognized in TLS point cloud data and recognized in the image was selected for model development and validation. Thus out of 202 trees, only 71 were used to develop the model. The developed model was then validated with independent test data set of 25 observations. The observed and predicted carbon was compared to determine the coefficient of determination (R^2) of model validation. Root mean square error (RMSE) was also calculated to assess model performance. RMSE illustrate the variation between observed values of carbon and predicted by the model. It is expressed in percentage as the ratio of RMSE and average observed carbon. Equation 6 shows the equation used to calculate RMSE.

$$\mathrm{RMSE} = \sqrt{\frac{1}{n}\sum_{1}^{n}(\mathrm{Cp} - \mathrm{Co})^2}. \quad \ldots\ldots\ldots\ldots\ldots\ldots\ldots\ldots\ldots\ldots \quad \text{Equation 6}$$

Where,
*C*p: Predicted carbon
*C*o: Observed carbon
n: Number of observations

3.3.10. Mapping AGB and Carbon Stock

The validated model was applied to estimate AGB and carbon of the whole study area; hence AGB/carbon stock map was generated to display the distribution of AGB/carbon in the study area using ArcGIS.

4. RESULTS

4.1. Image Segmentation

Automatic image segmentation of pan-sharpened image was performed using multi-resolution segmentation. As part of the process, several procedures were executed to create appropriate image objects representing real individual tree crowns.

4.2. Estimation of Scale Parameter

Estimation of Scale Parameter (ESP) tool was embedded to eCognition Developer 9.0.2. The tool was applied to find the most suitable scale parameter. Higher peaks in ROC-LV indicate the appropriate scales at which the image could be segmented. Figure 20 shows scale parameter of WorldView-2 satellite image in which scale parameter of 24, 34 and 39 were the suitable scales.

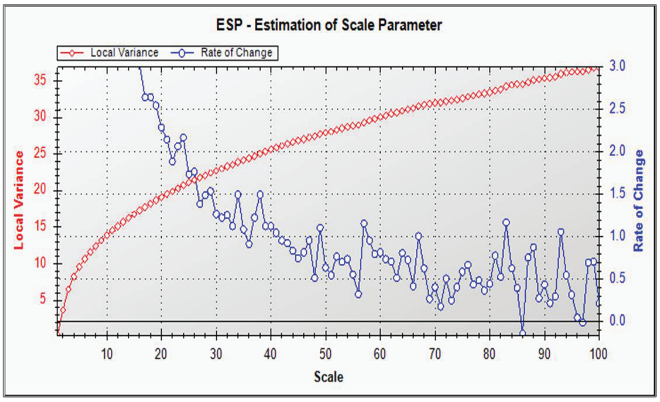

Figure 20: ESP tool of WorldView-2.

4.3. Multi-resolution Segmentation

Multi-resolution segmentation was applied with the scale parameters suggested by the ESP tool. Scale parameter 34 and 39 showed over segmentation of tree crowns. Apart from that, different smaller scale parameters i.e. 19, 21 were tried. However, these also tend to show under segmentation in most part of the image. The D-value was calculated to assess the accuracy of automatic image segmentation. The over segmentation and under segmentation value of scale 24 gave the acceptable result. Thus multi-resolution segmentation was finally done with the 24 scale parameter and 0.8 and 0.5 values for shape and compactness respectively. Part of the final segmented image can be seen in Figure 21.

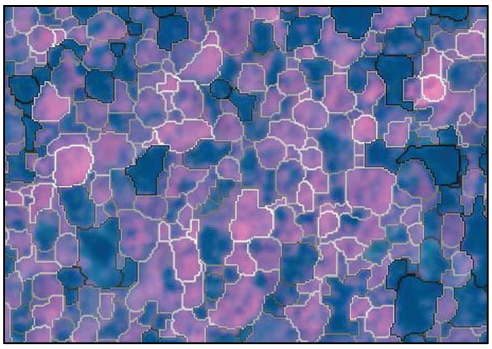

Figure 21: Sample of final output of the segmented image.

4.4. Segmentation Accuracy

Accuracy assessment of segmentation was done in two ways i.e. i) on the basis of 1:1 matching of segmented and reference polygons and ii) measure of "goodness of fit". Out of 279 manually delineated reference polygons, only 202 were matched one to one, which is 72% of matching. The over segmentation and under segmentation values for scale parameter 24 is 0.39 and 0.25 respectively hence, D-value is 0.32 (68%). Therefore the average accuracy of segmentation is 70%. Table 6 shows the summary of accuracy assessment. The results indicate that overestimation of tree crowns is greater than under estimation from automatic image segmentation.

Table 6: Accuracy assessment of segmentation

	Total reference polygons	Total 1:1 match	Over segmentation	Under segmentation	D-value
1:1	279	202			
Goodness of fit			0.39	0.25	0.32
Total accuracy		72%			68%

Figure 22: shows an overly of manually delineated reference polygons indicated with pink lines and their corresponding segments indicated with black lines.

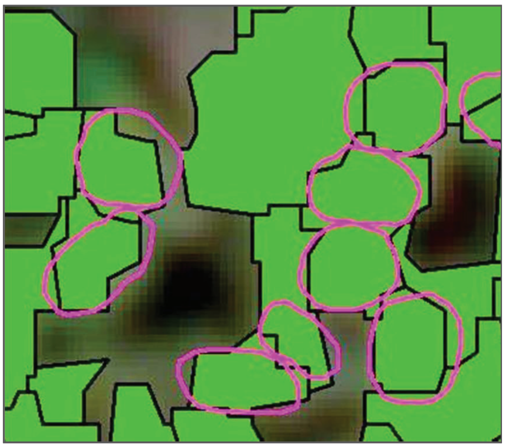

Figure 22: Reference and segmented polygons

4.5. Registration

Point cloud data from four different positions in every plot were aligned together using a minimum of three tie points. The coordinate of 2-D tie points pinned on the tree stem around the central scan position were created as corresponding points. The standard deviation of registered point cloud data ranges between1.01cm-4.21cm. In this way all three scan positions taken outside the plot were merged to the coordinate of the one taken from the centre of the plots. Figure 23 is a sample of registered points of a tree stem.

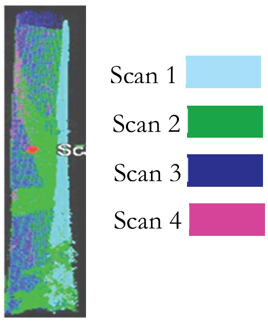

Figure 23: Sample of registered points of a tree stem from multiple scans.

4.6. Individual Tree Identification

Identification of an individual tree is a process of detecting points belonging to an individual tree stem (Liang et al., 2011). Identification of individual trees from point cloud data was done with the help of numbers tagged in the field. The tree stem was assumed as dense enclosed circular points which continue some meters of height and are separate from adjacent stem. In this way the trees which are clearly visible with marked number in the point cloud data were recognized as trees.

4.7. Individual Tree Extraction

The identified trees were extracted manually in RiSCANPRO. Totally 604 trees were recognized and extracted from point cloud data. Figure 24 shows sample of manually extracted trees.

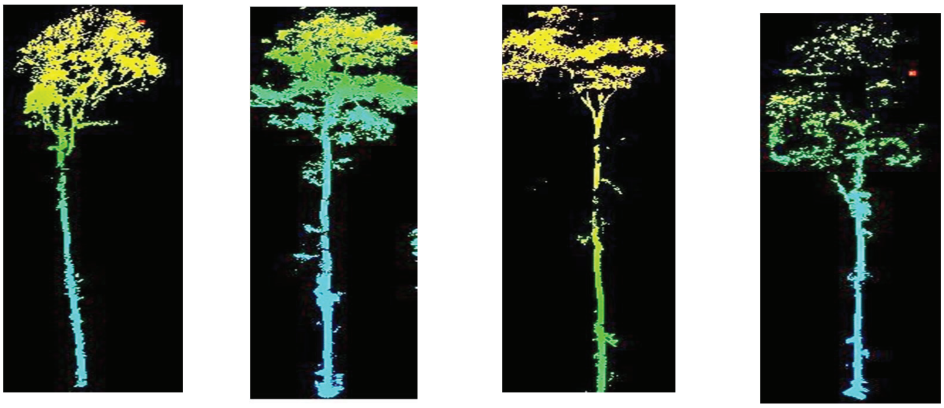

Figure 24: Sample of extracted individual trees in RiSCANPRO

4.8. Measurement of Height from Point Cloud Data

Tree height was measured as the difference between the lowest and highest point in the Z value of ASCII file. Each extracted tree from the polydata was exported to ASCII file (Figure 25) then the lowest and heights points were identified from the reading. Tree height of all the recognized trees (604 trees) was measured.

A	B	C
4.574	3.225	9.164
4.874	3.099	9.136
5.002	3.06	9.579
5.011	3.066	9.573
5.016	3.061	9.578
4.954	2.968	9.648
4.96	2.964	9.652
4.957	2.955	9.658
4.967	2.962	9.656
4.962	2.952	9.664
4.975	2.96	9.665
4.969	2.949	9.67
4.981	2.957	9.672
4.975	2.945	9.675
4.987	2.952	9.676
4.983	2.944	9.683

Figure 25: Tree height and Z-values (indicated with arrow) from ASCII file.

4.9. Measurement of DBH from Point Cloud Data

Measuring DBH was done manually using point to pint in RiSCANPRO software. The diameter at breast height (DBH) was determined at 1.30 m from visually identified lowest point of Z-value. Then point to point measurement was taken horizontally along the tree stem. Figure 26 shows the method how DBH is determined at 1.30 m and measured.

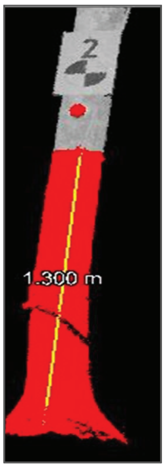

(A)

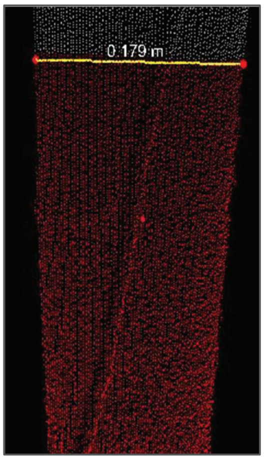

(B)

Figure 26: (A) Determined DBH at 1.30m and (B) Point to point measured sample of tree DBH

4.10. Descriptive statistics

A total of 32 plots were measured and recorded in field and scanned with TLS. However, measurements of 30 plots properly scanned with TLS and measured in field were used for further analysis. A total of 698 trees were collected from these 30 plots out of which 604 (86.5%) trees were identified and measured in the point cloud data. This means that 94 (13.4%) trees measured in the field were missed in the point cloud data. The number of missing tress in the plots greatly varies. Some of the reasons were blocking of the tagged number of the trees by the dense branches and limited returns (fewer number of points) from an object related to distance from the scanner. The detailed number of observations measured both in field and from point cloud data using TLS in each plot is given in Table 7.

Table 7: Number of tress measured in field and extracted from Point cloud data in each plot.

Plot. No.	Field recorded	TLS derived	TLS derived (%)	Missing trees	Plot. No	Field records	TLS derived	TLS derived (%)	Missing trees
1	12	12	100	-	16	26	25	96.1	1
2	19	17	89	2	17	29	23	79.3	6
3	16	12	75	4	18	13	13	100	-
4	9	9	100	-	19	28	25	82.1	3
5	15	15	100	-	21	25	25	100	-
6	30	14	46.6	16	22	26	25	96.1	1
7	26	18	69	8	23	30	25	83.3	5
8	22	22	100	-	24	16	15	93.75	1
9	11	9	81.2	2	25	26	21	80.7	5
10	24	20	83.3	4	26	32	24	75	8
11	29	23	79.3	6	27	24	17	70.8	7
12	29	23	79.3	6	28	22	19	86.3	3
13	28	28	100	-	30	22	21	95.4	1
14	33	32	97	1	31	35	33	94.2	2
15	18	18	100	-	32	23	22	95.6	1
Total									
plots	Field records		TLS derived		Missed trees		TLS derived (%)		Missing%
30	698		604		94		86.5		13.4

A normality test of the data distribution was assessed using SPSS statistics 22. Even though Okuda et al., (2004) mentioned that trees with >40 m height are common in primary forests of Peninsular Malaysia, one tree with 72.1m recorded in the field was excluded from the analysis based on our field observation including 17 other observations as an outlier hence, observations were reduced to 586. Height and DBH measurements from TLS were significantly different from a normal distribution, meaning that the p-value (written as sig. on Shapiro-Wilk of the table) is much smaller than 0.05 (Table 8). As it can be visually observed, relatively the distribution of TLS height was less skewed whilst TLS DBH is highly positively skewed (Figure 27). Since the study was using measurements from terrestrial laser scanner, only distribution pattern of these observations was displayed. The reader can also see distribution of field measured height and DBH provided in Appendix 3 and 4.

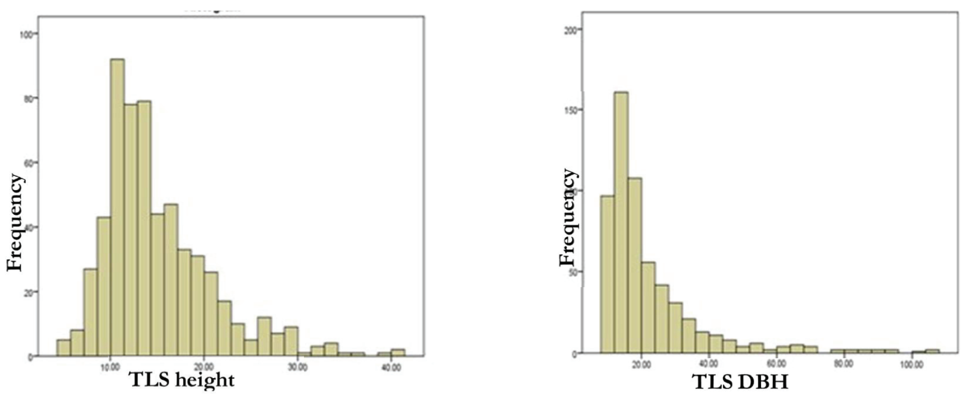

Figure27: Distribution of height (A) and DBH (B)

Table 8: Normality test of TLS observations

	Kolmogorov-Smirnova			Shapiro-Wilk		
	Statistic	df	Sig.	Statistic	df	Sig.
TLS DBH	.120	586	3.9592E-67	.904	586	1.295E-30
TLS height	.213	586	2.431E-17	.701	586	1.6233E-18

Throughout all the sample plots, 56 different tree species were identified in the study area. The most dominant tree species occurred in the area was *Syzygium* spp with 16% occurrence followed by *Vatica* spp and *Mastixia trichotoma* Blume with 15% and 10% of existence respectively. Each species of *Koompassia Malaccensis*, *Pimelodendron* spp and *Pimelodendron* spp occurred with 7% of the total composition followed by *Trypanosoma* spit 6% and Annonaceae 5%. The three different species in the area comprising 3% each were *Pentaspadon* motley, *Myristicaceae* and *Mallothus biaceae*. Among the dominant species, the least species identified in the area were *Shorea* spp with 2%. The rest of the species with less than 1% were grouped as 'others' consisting 16% of the figure. For better visualization the detailed distribution of the species is displayed in a pie chart in Figure 28.

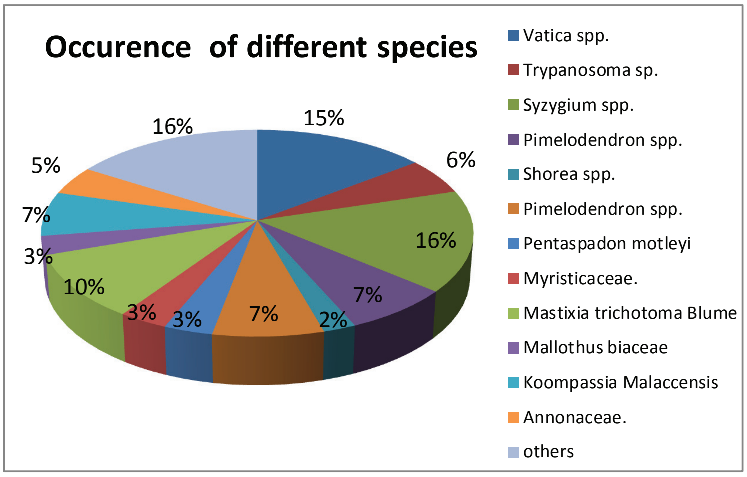

Figure 28: Occurrence of different species in the study area

4.11. Relationship of DBH and Height Measured from Field and TLS

Relationship of DBH and height measured from field and extracted from point cloud data was plotted to compare the relationship. The relationship of DBH from both measurements is linear and positive with R^2 of 0.96 and correlation coefficient (r) of 0.98 (Figure 29) whereas for height is also linear with R^2 of 0.75 and (r) 0.85 (Figure 30). In the upper part of Figure 30 some of tree height observations especially tall trees showed a deviation between these two measurements. Thus the relationship of field DBH and TLS DBH has stronger linear relation than field and TLS height. The correlation of both DBH and height from field and TLS was tested using Pearson correlation test which is found as significant ($P<0.001$) (Appendix 9). A summary of both measurements is shown in Table 9.

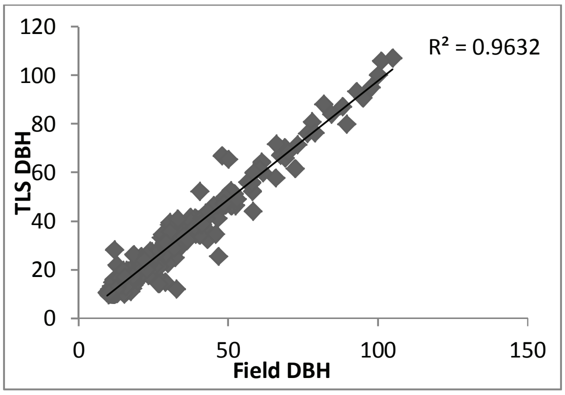

Figure 29: Scatter plot of field and TLS DBH

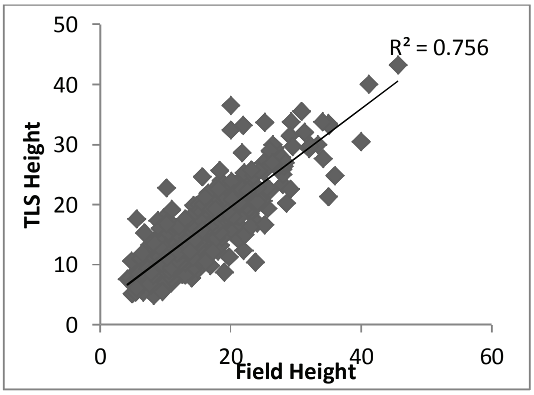

Figure 30: Scatter plot of field and TLS height

Table 9: A) summary of DBH

Statistics	Field DBH	TLS DBH
Minimum	10.40	10
Maximum	105.00	107.10
Mean	22.87	22.30
Standard deviation	15.75	15.70
Observation	586	586

B) Summary of height

Statistics	Field Height	TLS Height
Minimum	4.17	4.95
Maximum	46.00	40.25
Mean	14.50	15.04
Standard deviation	6.8	5.84
Observations	586	586

The summary of measurements shows that there is reasonable agreement between DBH and height from both measurements. The overall deviation of field and TLS measurements was analysed by calculating the RMSE. For DBH there was not much tendency of under or over estimation by the scanner since the RMSE was 2.9 cm (14.5% of mean DBH). However, in case of height measurements the RMSE was 3.3 m (20.7% of mean height). The trend of height measurement using TLS indicated a tendency to bias estimation especially for very tall trees observed in field. Moreover significance of the relationship between field and TLS measured DBH and height were assessed using paired t-test of 586 observations. First an F-test was carried out to calculate and find out if there is significant difference between these two data sets. According to the result of the F-test, relationship of both TLS derived and field measured DBH and height was statistically significant at 95% confidence level. Assuming the two variables have equal variances, a paired t-test was again used to assess the significance of the relationships. Results of t-test revealed that at 95% confidence level there is no significant difference in DBH and height measured from field and derived from TLS since t-calculated is greater than t-critical. Therefore the null hypothesis is rejected. Table 10 is showing the result of t-test for both DBH and height.

Table 10: A) Paired t-Test of height

Statistics	Field Height	TLS Height
Observations	586	586
df	585	
t Stat	3.45099	
P(T<=t) two-tail	1.02E-05	
t-Critical two-tail	1.964027	

B) Paired t-Test of DBH

Statistics	Field DBH	TLS DBH
Observations	586	586
df	585	
t Stat	4.6166518	
P(T<=t) two-tail	4.80E-06	
t-Critical two-tail	1.964027	

4.12. Plot-Wise Relationship of Field and TLS Measured DBH and Height

The deviation between field measurement and extracted from TLS was assessed for each plot (Table 11). DBH from both measurements was highly correlated since the correlation coefficient was greater than 0.86 except that plot 6 and 31 has (r) 0.66 and 0.74 respectively. On the other hand the RMSE of the two measurements ranges from 0.54 cm in plot 2 to 5.8 cm in plot 31.

Measurement of height from TLS and field also showed reasonable agreement in most of the plots. Nonetheless plot 2, 3, 6 7, 11, and 31 are among the plots with lower r and R^2 (Table 11) this means, these plots showed higher variability of height measurements. The rest of the plots have higher correlation values (r=>0.80). The RMSE of height measurements were higher as compare to DBH. Only few of the plots (1, 21, 22, 30, 32) has <1m mean height variation. The detail plot-wise comparison is below in Table 11.

Table 11: Plot-wise correlation analysis of field and TLS measurements of height (A) DBH (B)

A)

Plot. No	Height RMSE	RMSE %	r	R^2
1	0.93	7.6	0.98	0.96
2	3.1	33.19	0.76	0.58
3	2.3	27.8	0.67	0.45
4	1.3	15.8	0.86	0.74
5	1.3	10.4	0.90	0.81
6	3.14	30.66	0.35	0.12
7	4.8	35.4	0.55	0.43
8	4.3	22.1	0.89	0.80
9	2.3	13.4	0.96	0.92
10	5.1	35	0.88	0.78
11	3.5	32.4	0.60	0.36
12	2	15	0.94	0.88
13	3.3	23.3	0.88	0.79
14	5	35.6	0.82	0.62
15	3.5	23	0.80	0.65
16	2.2	12.7	0.93	0.87
17	2.8	19.3	0.90	0.82
18	2	14.2	0.85	0.83
19	3	19.3	0.93	0.87
21	0.8	5.4	0.98	0.96
22	0.8	5.9	0.99	0.98
23	2.8	18.6	0.83	0.69
24	1.9	13.9	0.93	0.86
25	2.2	15.4	0.89	0.79
26	1.9	11.2	0.95	0.91
27	2.1	9.5	0.83	0.69
28	2.1	12	0.97	0.94
30	0.5	3.8	0.99	0.97
31	4.3	31.6	0.58	0.33
32	0.8	5.9	0.98	0.97

B)

Plot. No.	DBH RMSE	RMSE %	r	R^2
1	1.43	6.7	0.98	0.97
2	0.54	4.6	0.91	0.83
3	1.42	8.1	0.98	0.97
4	1.44	9.7	0.99	0.98
5	1.6	9.3	0.97	0.95
6	2.7	21	0.66	0.41
7	1.4	9.9	0.97	0.95
8	2.8	12.6	0.96	0.93
9	3.3	12.2	0.99	0.98
10	3.1	10.25	0.99	0.98
11	4.1	20.5	0.93	0.87
12	1.4	4.6	0.99	0.98
13	1.4	6	0.99	0.98
14	2.2	9.7	0.86	0.93
15	1.3	6.2	0.99	0.98
16	1.4	5.2	0.99	0.97
17	3.8	15	0.98	0.96
18	2.2	9.2	0.99	0.96
19	3.8	13.7	0.96	0.93
21	2	9.1	0.99	0.98
22	1.3	6.3	0.99	0.97
23	1.1	5	0.99	0.93
24	3.1	12.2	0.98	0.98
25	4.1	16.7	0.97	0.94
26	1.4	5.9	0.99	0.98
27	3	12.6	0.95	0.91
28	3	11.4	0.98	0.97
30	1.44	5.53	0.98	0.96
31	5.8	22.8	0.74	0.56
32	1.5	6.6	0.98	0.96

4.13. Relationshiop 0f DBH and Height Estimated From CPA and Measured From Field

DBH and height was estimated from CPA to compare the relationship with field collected DBH and height thus if it can give reasonable carbon estimates. The correlation analysis of DBH and height estimated from CPA was plotted against field measured DBH and height to analyse the relationship. Tree height estimated from CPA (referred to as estimated height) was compared with field height. The resulting R^2 and correlation coefficient (r) was 0.26 and 0.51 respectively (Figure 31).The estimated values of height showed high variability as compare to field data. Similarly the correlation of DBH estimated from CPA (referred to as estimated DBH) with field DBH was not strong with the value of R^2 0.48 (Figure 32) and r of 0.69.

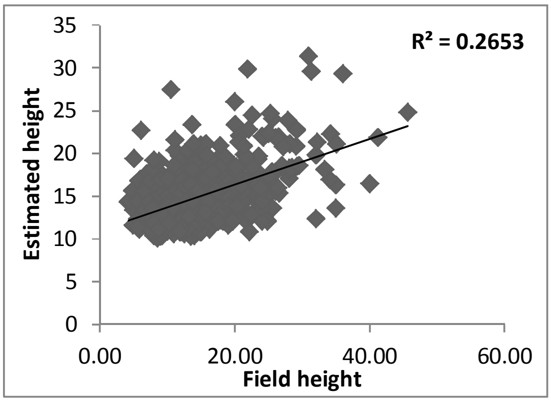

Figure 31: Scatter plot of Field and estimated height

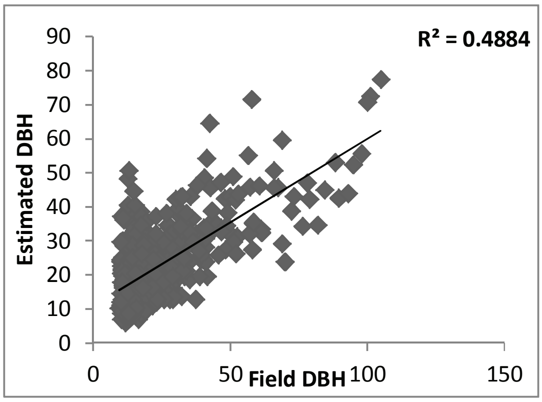

Figure 32: Scatter plot of field and estimated DBH

The significance of the relationship was assessed using paired t-test in Microsoft Excel. The result of the test indicated that DBH and height estimated from CPA was significantly different from corresponding field measured DBH and height since the t-calculated was smaller than t-critical. Therefore the research concluded that CPA doesn't give reasonable estimation of DBH and height as compare to ground truth field data. Table 12 and13 shows the detailed result of the t-test.

Table 12: Paired t-test of estimated and field heights

Statistics	Field Height	Estimated Height
Observations	586	586
df	585	
t Stat	-1.77283	
P(T<=t) two-tail	0.076777	
t-Critical two-tail	1.964027	

Table 13 Paired t-test of estimated and field DBH

Statistics	Field Height	Estimated DBH
Observations	586	586
df	585	
t Stat	1.485351	
P(T<=t) two-tail	0.137989	
t-Critical two-tail	1.964027	

4.14. Model Development and Validation

The total number of trees measured in field that were recognized in the image with one to one matching during manual delineation and identified in point cloud data were 202. Prior to model development outliers were removed based on the visual inspection with scatter plots and box plots thus, observations were reduced to 96. Then 71 observations from 25 different species were randomly selected for model development and 25 independent observations for validation. The analysis of the study is based on these

71 observations derived from TLS i.e. TLS-DBH and TLS-height (hereafter referred to as DBH and Height respectively). The descriptive statistics of the observations used for model development are presented in Table 14.

Table 14: Summary statistics of variables used for model development

summary statistics	Variables		
	DBH	Height	CPA
Mean	30.61	18.41	26.63
Standard deviation	12.67	7.04	13.315
Minimum	10.2	6.9	5
maximum	66	39.83	75
Observations	71		

Likewise for the 586 observations, normality test of the observations used for model development was also performed. The result depicted the distribution of DBH and CPA is significantly different from normal distribution ($P<0.05$) whereas observations of tree height were normally distributed (*i.e.* $P>0.05$) (Table 15. Considering the distribution of height of the whole data set (586 observations) which were nearly normal (Figure 27), the sample data sets of all observations selected for model development were considered as representative.

Table 15: Normality Test of DBH, height and CPA used for model development

	Kolmogorov-Smirnov[a]			Shapiro-Wilk		
	Statistic	df	Sig.	Statistic	df	Sig.
DBH	.136	71	.0001*	.891	71	.0000103
Height	.065	71	.200*	.974	71	.139
CPA	.128	71	.0006	.915	71	.000142

4.14.1. Relationship Among Independent Variables of AGB/Carbon Estimation

The strength of relationship among independent variables of carbon estimation was examined prior to model development. The relationship between DBH from TLS (hereafter referred to as DBH on the scatter plots) and CPA is non-linear with R^2 of 0.79 (Figure 33). On the other hand height from TLS (hereafter referred to as height on the scatter plots) and CPA is linear with R^2 of 0.68 (Figure 34). Relationship of DBH and CPA was close to linear. The relationship of both DBH and height extracted from TLS is also non-linear with R^2 0.50. More over the Pearson correlation coefficient of the variable CPA and DBH, CPA and height as well as DBH and height were 0.88, 0.81 and 0.71 respectively which is found to be highly significant ($P<0.001$) in all the relationships (Table 16).

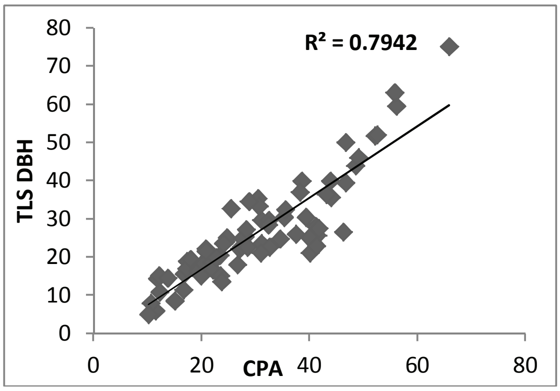

Figure 33: Scatter plot of TLS DBH and CPA

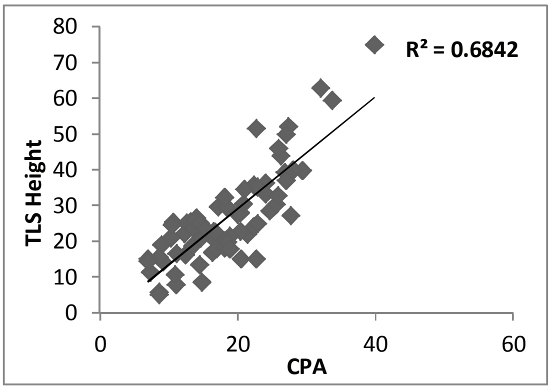

Figure 34: Scatter plot of TLS height and CPA

Table 16: Correlation test of DBH, CPA, and height

		DBH	Height	CPA
DBH	Pearson Correlation	1	.716**	.886**
	Sig. (2-tailed)		<.0001	<.0001
	N	71	71	71
Height	Pearson Correlation	.716**	1	.816**
	Sig. (2-tailed)	.<000		<.0001
	N	71	71	71

4.14.2. Graphical Analysis of Relationship between DBH, Height and Carbon

The study used measurements of DBH and height from TLS for analysis. After deriving the measurements of DBH and height from TLS, above ground biomass/carbon was calculated using an allometric equation (equation 4). Wood density of some species was identified from publications (King et al., 2005; Basuki et al., 2009) while average wood density of the identified species was assigned for the species missing from these publications. Correlation analysis of the independent variables used to calculate AGB/carbon with the dependent variable which is carbon was evaluated using Pearson correlation analysis. There is a strong positive relationship between DBH and carbon with R^2 0.92 (Figure 35) whereas R^2 with height is only 0.74 (Figure 36). These results indicates that 92% and 74% of carbon was explained by DBH and height respectively extracted from TLS. Comparatively extracted tree height has lower relation with calculated carbon.

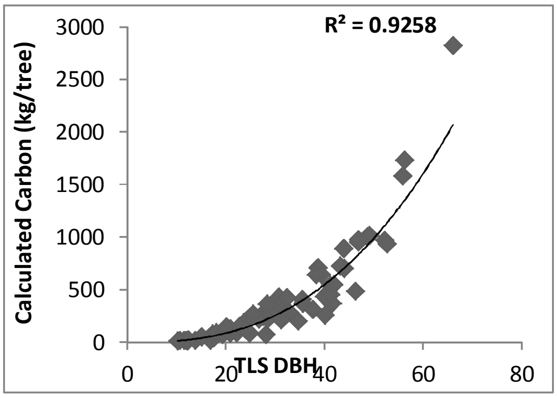

Figure 35: Scatter plot of DBH and carbon

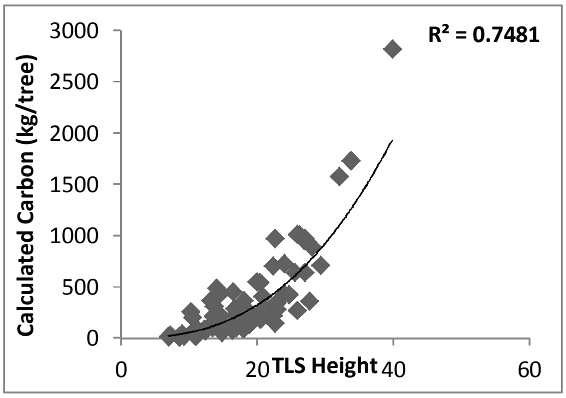

Figure 36: Scatter plot of height and carbon

Significance test of correlation between DBH-carbon and height-carbon was done and was found to be significant (P<0.001). Correlation of 0.96 and 0.80 were obtained between carbon-DBH and carbon-height respectively (Table 17).

Table 17: Correlation test of independent and dependent variables

		DBH	Height	Carbon
DBH	Pearson Correlation	1	.716**	.963**
	Sig. (2-tailed)		<.0001	<.0001
	N	71	71	71
Height	Pearson Correlation	.716**	1	.803**
	Sig. (2-tailed)	<.000		<.0001
	N	71	71	71

4.14.3. Model Development

4.14.3.1. Relationship between CPA and Carbon

Developing a model was done in two ways: one was a multiple regression model developed using TLS derived height and CPA as independent variable and the other was using only segmented CPA. This was mainly done to evaluate the combined effect of height derived from TLS and CPA on improved estimates of carbon. Prior to that, the correlation of segmented CPA and observed carbon was established. The relationship between CPA and carbon was non-linear with a correlation coefficient of 0.91 and R^2=0.80 (Figure 37). The significance of the relation was also verified at 95% confidence level with one-way ANOVA (Table 19). Correlation of height and carbon as well as CPA and height was presented in section 4.13.2 and 4.13.1 respectively.

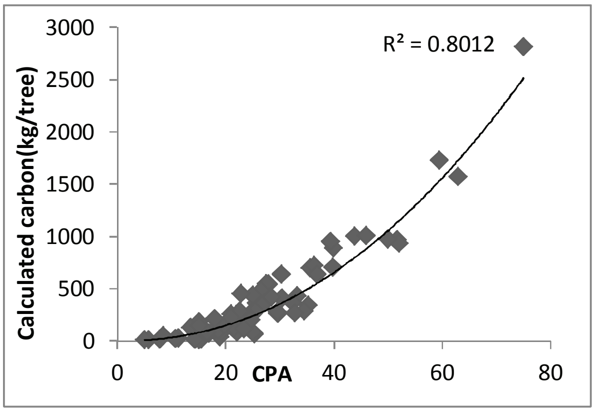

Figure 37: Scatter plot of CPA and carbon

4.14.3.2. Modelling Carbon from CPA and Height (Multiple Regression)

To check multi-collinearity between the two explanatory variables of multiple regression (i.e. CPA and height), a collinearity test was executed where variance inflation factor (VIF) was less than 10 (3.167) and no sign of multi-collinearity was found (Appendix 2). As mentioned in section 4.13, CPA data was not normally distributed thus log transformation was applied using natural logarithm (ln). Data transformation was aimed to normalize the distribution and fitting the data to the model. Hence, a multiple regression model of log-transformed data was established between height and CPA as explanatory variables and calculated carbon as response variable using 71 observations (Table 18). The model resulted in values of 0.85 and 0.92 for the coefficient of determination and correlation coefficient respectively. This demonstrates that the 85% of observed (calculated) carbon was in agreement with CPA and height. One-way ANOVA was employed to calculate the significance of R^2 of the model. The result shows that the model is found as significant. A summary of the regression analysis is presented in Table 18.

Table 18: Regression analysis of CPA, height and carbon

	Coefficients	*Standard Error*	*t Stat*	*P-value*
Intercept	-520.6854368	61.16917136	8.51222	2.58E-12
TLS Height	8.913118647	5.495862771	1.621787	0.009477
CPA	28.11780744	2.907290809	9.671481	2.1E-14

ANOVA

	df	*SS*	*MS*	*F*	*Significance F*
Regression	2	12797397.69	6398699	193.3689	8.74E-29
Residual	68	2250162.725	33090.63		
Total	70	15047560.42			

Regression Statistics	
Multiple R	0.926245345
R Square	0.857930439
Adj. R Square	0.853751923
Standard Error	177.3083181

A model was developed to estimate carbon stock based on the regression results (Equation 7)

Ln **Carbon= -520.68+8.91****Ln***Heigh+28.11****Ln*** **CPA**……………………….Equation 7

4.14.3.3. Validation of Multiple Regression Model

Multiple regression model was validated by plotting the carbon predicted from CPA and height against the observed carbon, using 25 independent data sets. The resulting coefficient of determination was 0.87 (R^2= 0.87) (Figure 38). This means that about 87% of carbon calculated from TLS height and CPA was explained by the developed model. To check the error of estimation, RMSE of the validated model was also calculated to be 26.6%.

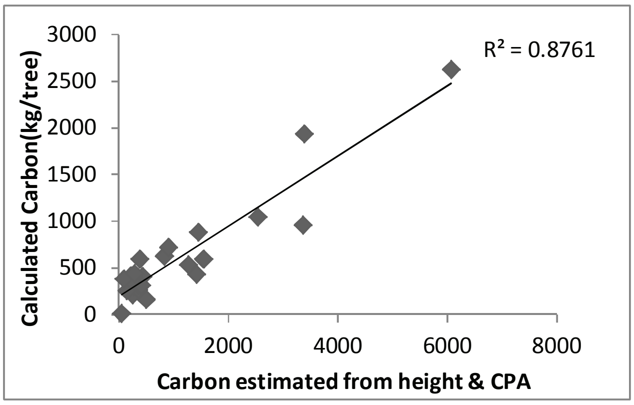

Figure 38: Scatter plot of multiple regression model validation

Even though the accuracy of multiple regression model is acceptable, the possibility of estimating carbon stock is limited to the sample plots scanned with the sensor. In other words it is not possible to have carbon estimation of the whole study area and map the distribution since height data is not obtainable with terrestrial laser scanner. Therefore the study aimed to develop a second model for estimating and mapping carbon stock in the study area using only crown projection area (CPA) available for whole area.

4.14.3.4. Modelling Carbon from CPA (Non-Linear Model)

Regression analysis was carried out using CPA only resulting a coefficient of determination of 0.80 (R^2=0.80). Since it is more relevant with higher R^2 the non-linear model *i.e.* quadratic model was preferred than simple linear model. The correlation coefficient of the CPA and carbon was also high (0.84) indicating strong correlation between the variables. According to the one-way ANOVA, the model is significant at 95% significance level. The summary of regression of the developed model for carbon stock estimation in the study area is in Table 19.

Table 19: Regression analysis of CPA and Carbon

	Coefficients	*Standard Error*	*t Stat*	*P-value*
Intercept	-326.8605298	71.08605815	4.5981	1.91E-05
CPA	20.76154776	4.744808143	4.375635	4.27E-05
CPA^2	0.196555196	0.078046629	2.518433	0.014146

ANOVA

	df	*SS*	*MS*	*F*	*Significance F*
Regression	2	12909760.12	6454880	205.3194	1.53E-29
Residual	68	2137800.297	31438.24		
Total	70	15047560.42			

Regression Statistics	
Multiple R	0.849064367
R Square	0.80467931
Adj. R Square	0.802428286
Standard Error	184.0446332

Based on the summary obtained from regression analysis (Table 19), a model was developed to estimate carbon stock of the study area (Equation 8).

***Ln* Carbon= -326.86+20.76**ln*CPA+0.19**ln*CPA^2** ……..……….….…… Equation 8

4.14.3.5. Validation of Non-Linear Model

The non-linear model was validated with observed and predicted carbon plotted against each other using the same data set as for the multiple regression model (25 independent observations). The depicted coefficient of determination was 0.84 (R2=0.84) (Figure 39). This indicates that about 84% of carbon calculated from TLS data was explained by the developed model. The calculated RMSE of the model was 29.3%.

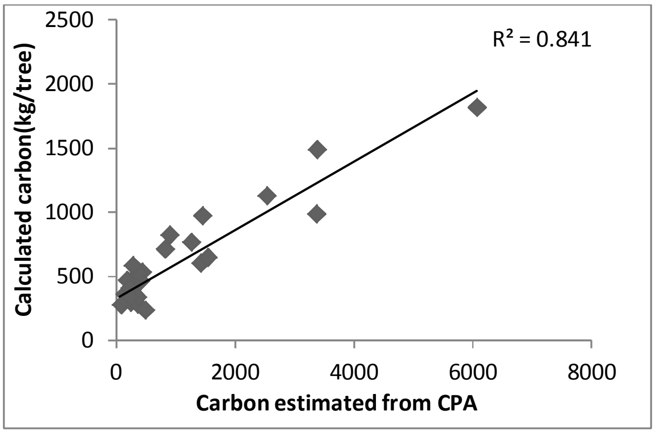

Figure 39: Scatter plot of non-linear model validation.

4.14.4. Carbon Stock Mapping

The non-linear model for CPA and carbon gave reasonable results. Therefore, was used to estimate the amount and map the distribution of carbon stock in the study area. The estimated above ground biomass in the area was 1,355,574.2 Mg within around 3,442 hectare of area covered by the study area (part of the whole BRFC of 117,500 ha). This means the amount of AGB was estimated to be 393.82 Mg per hectare. Above ground biomass was converted to carbon stock using conversion factor (0.47). Thus the total amount of carbon in the area was estimated to be 637,119.87 Mg. Therefore the estimated amount of carbon per hectare in the study area was 185 Mg ha^{-1}. The quantity of estimated carbon ranges from less than 500Kg/tree to greater than 2000kg/tree: where most of the trees had <500kg whilst few of the tress had >2000kg of carbon per tree. The variation in carbon amount was inspected, and it was concluded that the carbon per tree is more related with the size of CPA. Most of the trees with more than 2000kg are those with large CPA. The carbon stock map of the study area is shown in Figure 40.

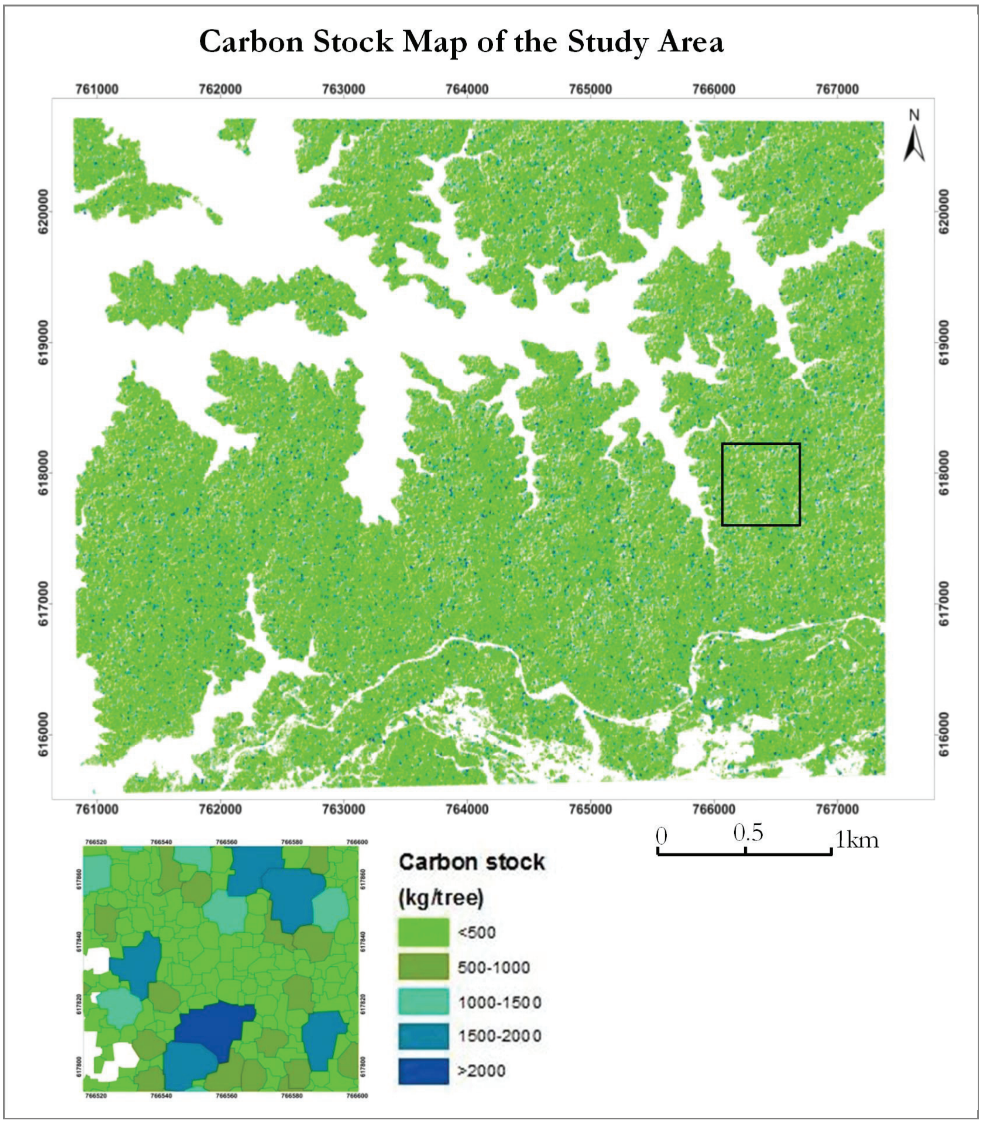

Figure 40: Carbon stock map of the study area

5. DISCUSSION

5.1. Distribution of TLS Data

The distribution of 586 tree heights and diameters extracted from point cloud data showed high skewness value for diameter at breast height whereas nearly a normal distribution for height. Skewness indicates lack of symmetry of data distribution as it tilts to the left or right of the centre points (Geer & Wegkamp, 2012). In a probability distribution, the data can be positively (long tail in the positive direction) or negatively (long tail in the negative direction) skewed (Doane & Seward, 2011) (Figure 41). In case of our study the variables were skewed positively. The possible reasons for high skewness of DBH could be that measurements were taken for trees with a DBH greater than 10 cm (since these with less than 10 cm add insignificant amount of biomass) and if trees with less than 10 cm would have measured, the distribution would be close to normal. More over in the naturally regenerating, protected and old tropical forest of the study area, DBH is expected to have wider distribution as mentioned by Karna, (2012). In case of height, even though it is not highly skewed, it portrayed variation in distribution. As indicated by Okuda et al. (2004) trees that are taller than >40m are common in tropical rainforest of peninsula Malaysia indicating wider distribution in height as well.

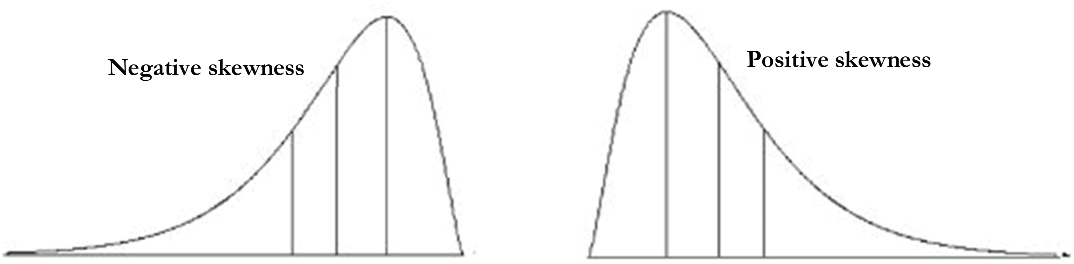

Figure 41: Graph of positive and negative data skewness (Doane & Seward, 2011)

5.2. Segmentation Accuracy

The accuracy of individual tree crown segmentation using multi-resolution approach was evaluated in two ways. It resulted in 72 % of accuracy using one to one matching of manually delineated polygon as a reference to automatic segments by the software. The overlap of segmented and reference polygons was considered as one to one if it is more than 50% as stated by Zhan et al. (2005). Whereas 68% of accuracy was obtained using calculated "goodness of fit" measure. Hence, the overall accuracy of segmentation is 70%, which implies a segmentation error of 30%.

The segmentation accuracy achieved in this study is 72% using 1:1. This is lower than the study by Wang et al. (2004) and Koch et al. (2006) which obtained 75.6% and 87.3% in detecting tree crown of coniferous and deciduous forests respectively and Baral (2011) who got 74.4% of segmentation accuracy in tropical forest of Nepal using Worldvew-2. Similarly Erikson, (2011) achieved 73% of 1:1 correct correspondence of polygons in naturally generating mixed forest using aerial image. Our study obtained higher accuracy than that of Ke & Quackenbush (2008) who achieved 61.3% of segmentation accuracy using region growing algorithm in mixed forest. While making comparisons, the difference in conditions under which the study is taken, varying spatial and spectral resolution of images, species and forest type are among the most important factors to be considered (Brandtberg & Walter, 1998).

The study applied multi-resolution segmentation of tropical rain forest with complex canopy structure and species composition of different ages. In such dense natural forest, intermingling multi-layers of canopy and variation of illumination within or between tree crowns are common (Figure 42)

. Therefore, segmentation approaches which consider the top of tree crown as the seed with brightest spectral value (Culvenor, 2002; Wang et al., 2004) are not suitable. Because, unlike coniferous trees crown with pointed top and most possibly to have one tree top, in the tropical forests it is possible to have one tree top characterized by large multiple branches with a non-conical shape of tree crown (Figure 41). Rather multi-resolution segmentation is most applicable approach as it uses spatial and spectral homogeneity of pixels to merge in to image object (tree crown). Moreover multi-resolution segmentation is appropriate algorithm to segment heterogeneous forests (Kim et al., 2008) and is proved by Lamonaca et al. (2008) as a powerful method to extract meaningful information from high resolution images with heterogeneous forest attributes.

Figure 42: Multi-layers of canopy in tropical rainforest

(Source: http://www.stri.si.edu/english/research/facilities/terrestrial/cranes/forest_canopies.php)

In multi-resolution segmentation, the size and homogeneity of image objects is determined by the scale parameter (Definiens, 2012). As categorized by Benz et al. (2004) scale parameter can be fine, medium and course. Course scale is practical for extracting forests and open land scape and medium scale is used for group of aggregated buildings to several medium scale settlements. Whereas fine scale is suitable for segmenting smaller image objects such as trees, buildings and roads. Since this study was aimed at segmenting individual tree crown and the image includes a road with some small paths, a fine scale of 24 scale parameter resulted in an optimum fit of automated segments to those of manually delineated reference objects with 0.25 and 0.38 under- and over-segmentation. Over-segmentation is relatively higher than under-segmentation in this study. This means that the automated segments exceed the area of reference polygons. Over-segmentation of image is associated to the presence of noise resulting over detection of boundaries by morphological gradient (Carleer et al., 2005). Over-segmentation can be avoided by applying filtering to smooth and locally homogenize the gradients within a crown (Ke & Quackenbush, 2011; Carleer et al., 2005). Therefore, a low pass 5*5 filter was applied in this study to minimize over-segmentation.

5.3. Processing Point Cloud Data

5.3.1. Multiple Scan

Measuring forest parameters using TLS involves either a multiple or a single scan. In a single scan, trees are scanned from a single position usually from the centre providing limited details from one side view of objects. The advantage of single scan is fast and easy thus, saves scan time during field work and since there is less number of points, it also take less time of data processing (Bienert et al., 2006). Whereas in a multi-scan, the scanner acquire full coverage of the tree surface from several scan positions (in and out of the centre). Registration of multiple scans was done to merge the points with different position into common position (global coordinate) using artificial objects as a reference targets (section 3.3.6.1). Multiple scan is better than single scan because it provide a full portrait of tree parameter from merged point clouds (Liang, 2013)(Figure 43). Several researches (Huang et al., 2008; Hopkinson et al., 2004) used multiple scan approach in the field of forestry.

Figure 43: Sample of multiple scan representing 3-D scene of objects.

5.3.2. Tree Height Measurement

Measuring tree height directly from Terrestrial Laser Scanner is very difficult in dense sample plots of tropical rainforest. The problem lies in capturing tree tops in mostly overlapped canopy and shadowed by the lower canopy layers and branches which does not allow the sensor to detect the top part of the tree or result in low density of points in the upper part of the tree which introduce errors (Figure 44). Particularly in some very tall species of trees having wider crown, the influence of underestimation by TLS was observed.

Figure 44: Less density of points on top part of the tress

Figure 45: Dense canopies resulting difficulties to capture actual tree height with TLS.

Depending on the tree height, forest density and slope of the plot the difference in tree height between field and TLS varied from 0.5 to 5.1 m among the plots (Table 11). The average RMSE of tree height measurements of 586 trees is 3.3 m (20.7% of mean tree height). The study by Hopkinson et al. (2004) experienced similar problems and reported around 1.5m underestimation of tree height by the sensor applying multiple scan approach. The variability of heights in our study is higher than that of Hopkinson et al. (2004). However, the two studies are different in two ways. Firstly, Hopkinson et al., (2004) carried out the research in both deciduous and red pine plantations with no understory and effect of canopy layers as compare to our study. Secondly, his study compared only 9 trees in two plots. Furthermore, Maas et al. (2008) found a RMSE of 4.55m when comparing field measured and automatically derived tree heights using both multiple and single scan approach of 4 plots (9 tress).

In field height measurement as well, there was an obstruction of the top or bottom view by the foliage of the trees, Liana (climber), palm and Bamboo etc. (Figure 46) and other several causes such as misreading of actual tree height in case of tilted trees (Figure 46, B). In addition to this, using conventional tools the assumption of geometry in height measurement is right angle triangle which may not be practical in undulating terrain of the study area (Figure 46 A). These can systematically introduce error of over or under estimation of field height measurements.

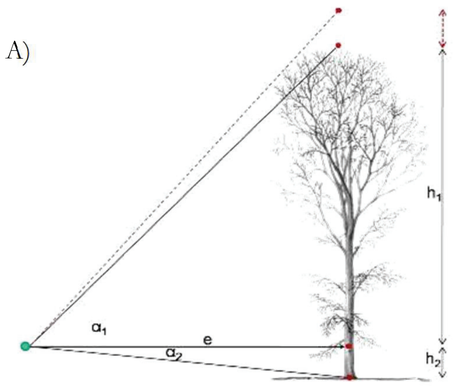

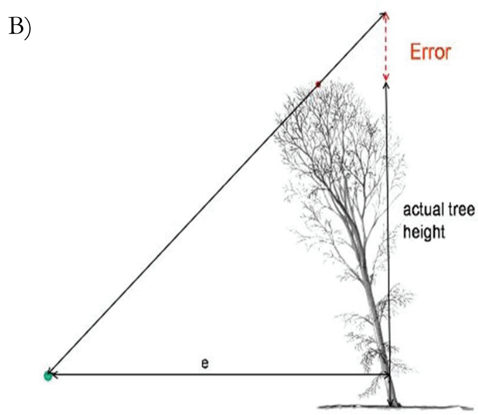

Figure46: Errors in measuring actual tree height.

(Source: http://wiki.awf.forst.uni-goettingen.de/wiki/index.php/Tree_height)

Figure47: Dense undergrowth of trees blocking the view.

5.3.3. DBH Measurement

Diameter at breast height is one of the most important tree parameters in forest inventory of biomass estimates since it explains about 95% of variation in aboveground biomass/carbon (Brown, 2002). One of the most important steps of measuring DBH in the field is to determine the diameter at breast height of the trees at 1.30 m. However, determining DBH exactly at 1.30 m from the tree base is not always practical. This is due to: firstly, different person determines the diameter at breast height of the tree based on his or her own height. Secondly, the base of a tree may not be levelled always in this case the DBH of the tree will be more or less than1.30 m. Furthermore, there is variation in precision of DBH measured with different instruments such as diameter tape and calliper. These factors influence the measurement of DBH to be subjective. The above mentioned errors are reduced in case of TLS, because the subjective errors such as different measuring person and variation in measuring device are excluded (Simonse et al., 2003). In addition to this manual errors involved in reading and recording are eliminated. The advantage of using TLS on minimizing subjective errors is discussed by Simonse et al. (2003).

The correlation of field measured and TLS derive DBH was analysed by calculating the coefficient of determination which was found to be highly correlated. The variability of the measurements was assessed treating each plot separately. The variation ranges between 0.54 cm to 5.8 cm and on average the overall deviation of both measurements was 2.9 cm (14.5%of mean DBH).

5.4. Relationship Among Independent Variables for Modeling AGB/Carbon Stock Estimation

In natural broadleaved deciduous forests, the relationship of DBH and CPA exists is non-linear since the rate of tree stem keeps growing while CPA stabilizes with age due to the intense competition among neighbouring tree (Shimano, 1997). Hemery et al. (2005) pointed out that relationship between CPA and DBH is close to linear with trees 20 cm-50 cm in species of broadleaved trees. This is practical in our study, due to the fact that most of observations were with DBH less than 50cm (Figure 27) and the mean DBH of trees were 22.30 cm (Table 9), the relationship between DBH and CPA was found to be non-linear but very close to linear with R^2 value of 0.79. The study by Shah, (2011) derived higher and a linear correlation of 0.83 for *Shorea rubusta* in Nepal. In addition to this, the study carried out in deciduous and coniferous forests by Shimano, (1997) obtained non-linear relationship of R^2 0.93 and 0.85 between DBH and CPA measured in the field for deciduous and coniferous trees.

On the other hand the relationship of tree height and DBH was also non-linear with R^2 0.50 which is not high. In areas with complex forest conditions such as species diversity, slope, aspect and altitude, this complexity result in inaccuracy and a complex relationship of height and DBH (Temesgen et al., 2005; Fang & Bailey, 1998). The observations used to develop the model were from 25 different species which represent the whole data set. In such diverse and dense forest the growth characteristic of tree species varies. Some species can advance their growth in height more rapidly while others tend to maintain their development in DBH or vice versa depending on the species. This could tend to lower the relationship. Likewise, the relationship of CPA and height is linear with 0.68 coefficient of determination. The crown size increased as height of tree increases in a linear fashion. The ratio of crown diameter to tree height is affected by competition measures (e.g. density, crown competition), tree size (e.g. age) and site (e.g. slope, elevation, aspect) (Temesgen et al., 2005).

5.5. Model Development

5.5.1. Correlation Analysis between DBH- Carbon and Height-Carbon

A correlation coefficient of variables >0.7 or <-0.7 is considered to indicate a strong relationship (Clemens et al., 2008). Emphasizing on coefficient of determination that exist between empirical relationship of variables, correlation of independent variables (DBH, height) and dependent variable (carbon) were analysed. The relationships were all non-linear and significant ($P<0.001$). The result showed that the variable DBH was highly correlated with carbon (R^2= 0.92). The result is comparable with the value of R^2=0.98, obtained by Ilyas (2013). In fact, this result may be expected since DBH is one of the most important parameters, explaining about 95% estimate of forest biomass/carbon (Gibbs et al., 2007). The amount of carbon in this study increased with DBH (Figure 35). However, the rate of increment in DBH is at lower rate in the trees with larger diameters and so does the relationship is non-linear with carbon. Even though the stem of a tree continue to grow, it does at slower rate with increasing age. Similarly, height and carbon demonstrated a strong and significant ($P<0.001$) non-linear correlation (R^2=0.74). The correlation coefficient is 0.80. The result is in agreement with the study by Karna (2012) who obtained value of 0.74 for R^2 and 0.86 for correlation coefficient for the species *Terminalia tomentosa*. The value was lower for the other four species in Karna's study.

5.5.2. Modelling the Relationship between CPA and Carbon

Non-linear regression was established using observed carbon as the dependent and log-transformed CPA as the independent variable to develop a model. Since the rate of increase in size of tree crown stabilizes while the tree continues to grow, the rate of increase in carbon also decreased at lower rate (Figure 37). The coefficient of determination of the model was 0.80 and relationship with carbon was significant. A reasonable accuracy of segmentation is one of the reasons for the high coefficient of determination. Improved segmentation accuracy (77%) and higher coefficient of determination (R^2=0.88) between observed carbon and crown projection area of mixed species was achieved in the study by Baral, (2011) in a sub-tropical forest in Nepal using Geo-Eye imagery. Singh, (2014) obtained similar result (R^2 =0.78) to our study while modelling carbon stock of Sal (*Shorea robusta*) using WorldView-2 in Doon Valley, India. The result obtained by Sumarah (2014) was lower than the result achieved in this study due to the low segmentation accuracy according to the author's discussion.

The coefficient of determination of the validated non-linear model was 0.84. This means that the model explained 84% of predicted carbon. Improved R^2 of model validation is in agreement with the segmentation accuracy and higher number of observations was used. However the model introduced 29.3% of error (RMSE= 29.3%).

5.5.3. Modelling Carbon from Height and CPA

Multiple regression was applied using height from TLS and CPA from the image as explanatory variables to develop a model and estimate carbon stock of individual trees in the sample plots. Both explanatory variables were highly correlated to observed carbon and variance inflation factor (VIF) was less than 10 with no existing multi collinearity between them. Multiple regression model was preferred to get the improved prediction of carbon (Ketterings et al., 2001) as well as higher coefficient of determination (Cairns et al., 2003; Brown, 2002) from combined effect of two explanatory variables than one. The log transformed data was used to develop the multiplicative model.

The resulting coefficient of determination of the model validation was 0.87 with RMSE 26.6% indicating how accurately carbon can be estimated from the model. Higher output of the model validation was a combined effect of height and CPA which can enhance least variability between observed and predicted carbon. The result is higher as compare to the study by Nguyet, (2012) who developed multiple regression model for *Shorea robusta* with R^2 0.68 validation accuracy using CPA and height derived from GeoEye image and Airborne Lidar respectively. It is also lower than a species specific model developed for *Shorea robusta* by Karna (2012) who obtained a coefficient of determination of 0.94. On the other hand, the study assessed whether including tree height improves model accuracy or not. Rutishauser et al. (2013) achieved R^2 of 0.96 with tree height included in the plot wise biomass estimation using the generic allometric equation developed by Chave et al. (2005).

Therefore from our study it can be concluded that applying multiple regression using height form TLS and CPA from image predicted more accurately than CPA only. However height from TLS is operational for plot-wise inventory only. Thus the non-linear model developed using CPA was used to map carbon stock of the study area. For possible solutions to accurate estimates of carbon for the whole study area, a combination of Airborne Lidar derived height and TLS derived accurate tree position is suggested.

5.6. Carbon Stock Estimation

The amount of above ground biomass in the study area was estimated to be 393.82 Mg ha^{-1} that is, 185 Mg ha^{-1} of carbon stock. Our study estimated an amount comparable to that which is found in the study by Laumonier et al. (2010) in hill *Dipterocarp* old growth tropical rain forest of south and central Sumatra. They found a range of 135-240 Mg ha^{-1} of carbon stock with a mean of 180 Mg $ha\text{-}^{1}$ using a generic allomeric equation by Brown (1997). On the other hand, Dirocco (2012) estimated 146 Mg ha^{-1} of carbon in a very close site of Temenger forest reserve which is poorer than our study. The result of this study is within estimated range of above ground biomass in tropical rain forest of Asia which is 120-680 Mg ha^{-1}(IPCC, 2006). One should keep in mind however, that the environmental condition of the study area, the allometric equation used and methods applied could result in variations of the estimates.

5.7. Source of Errors and Uncertainities

Errors can be propagated during data collection, processing and analysis (Wang et al., 2005). In this study mostly error related to segmentation, an allometric equation used and point cloud data influenced the developed model hence, the carbon map.

5.7.1. Errors Related To Image Segmentation

Time difference

The image was acquired in February 2013 and filed data were collected during September 2014. Tree crown may grow during the time lag and appear different resulting variation in estimated and measured crown as stated by Song et al. (2010).

Viewing angel

Quality of satellite image is subjected to several uncontrolled factors which induces misinterpretation. Among these; viewing angel of the sensor and sun angle plays a key role in top view projection of canopy area as in real situation. In an ideal situation where the sun should be over-head (0^0 with reference to Zenith or 90^0 with reference to the horizon) and the sensor looks down straight vertically (nadir view), thus providing the true representation of tree crowns. Higher off-nadir view and low sun elevation angle results in slanted projection of objects causing misinterpretation and errors.Viewing angle of the image in this study was 22.30^o off-nadir which can considerably distort the appearance of circular tree crown as elongated i.e. different from the reality. In addition to this, sun angle during image acquisition (74.80^0), affects the precision of segmentation by increasing amount of shadow detected by the sensor. Similar effects of off-nadir viewing angel and topography was discussed in the study by Song et al. (2010). Figure 48 shows overview of tree crown under three different perspective of sun angle and view angle.

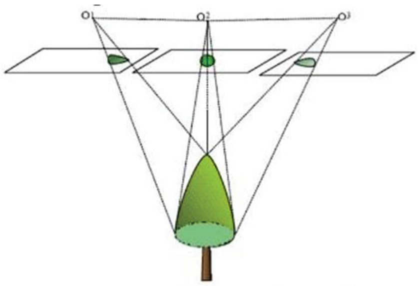

Figure 48: Tree crown from three different views (Li et al., 2008)

Forest conditions

In the photo-synthetically active forest of the study area, a high density of understory and proximity of crowns was observed during field work limiting the algorithm to separate individual crowns as mentioned by Erikson (2011) and Bunting & Lucas (2006). Figure 49 shows the dense and overlapping condition of the forest in the study area.

Figure 49: Dense and overlapping condition of forest in the study area (WorldView-2 image).

5.7.2. Allometric Equation

Using an allometirc equation avoids destructive method of forest inventories as it relates the biomass /carbon of trees to easily measurable variables. The existing allometric equations vary with forest type. Some are local and species specific whilst in complex forests, mostly in tropics the equations are more generic in nature (Brown, 1997). The generic equation developed by Chave et al. (2005) was used in this study. Generic allometric equations used are categorized as ecological regions (e.g. wet, dry, moist), consider numerous trees with range of variability in diameter which improves precision of the equations and are less biased (IPCC, 2007). However, generic equations may not represent the true biomass of trees. For equations not developed for specific sites, particularly *a* and *b* parameters vary across sites. Therefore, variation in these variables could be source of uncertainty in biomass estimation (Ketterings et al., 2001).

5.7.3. Errors Related To Sensor and Form, Nature of Scanned Objects

Laser scanners detect objects by measuring laser beam reflected back from the surface of an object. The strength and amount of returned back signals is influenced by reflective ability of objects' surface (Cosarca et al., 2009) and other factors such as distance from the sensor. As the distance (vertical and horizontal) between scanner and target object increase the quality and density of points decrease (Hopkinson et al., 2004) In this case, the amount and strength of reflected signals in dark plots (very dense canopy cover) or distant objects were weak. This in return was affecting the precision of point measurements in some trees.

In some cases temperature of the scanner may exceed the external temperature due to internal heating of the sensor components (internal factor) in addition to sunlight (external factor). These factors could be the cause of distortion (noise) of point cloud data in few plots as explained by Cosarca et al. (2009). The study applied four scans to get enough coverage of tress from different positions. However, there existed some part of trees covered from less than four scan positions. These resulted in missing information and uncertainties such as unclear edged of the stem, indefinite tree height particularly with trees far from the centre and other scan positions. To avoid such uncertainties reducing the radius of the plot or increase the number of scans is suggested.

5.8. Limitations of the Research

1. Even though the research applied ESP tool to determine suitable scale parameter, the trial and error way of discovering the appropriate scale was also done which takes time and hardly finds the right scale of multi-resolution segmentation.

2. Point cloud data processing is time consuming.

3. Because of its weight the terrestrial laser scanner was not easily manageable to carry and operate in the steep slopes of the study area.

4. If airborne lidar data would have been available, the study could apply multiple regressions of height and CPA with improved model accuracy to estimate carbon stock of the whole study area.

4. TLS can provide 3-D measurement of forest parameters efficiently. However, automatic extraction of point cloud data was an algorithmic challenge.

6. CONCLUSION AND RECOMMENDATIONS

6.1. Conclusion

In this study a method was developed with a combined data from terrestrial laser scanner and high resolution satellite image to estimate carbon stock in tropical rain forest of Malaysia, Royal Belum State Park as a case study. The regression model developed with DBH and height from TLS and crown projection area from very high resolution satellite image using object base image segmentation was the main technique of the study. There was a non-linear relationship between independent variables (CPA, DBH, height) of estimating carbon stock and dependent variable (carbon). Correlation coefficients were 0.91(R^2=0.80), 0.96 (R^2=0.92) and 0.80 (R^2=0.74) for CPA-carbon, DBH-carbon, height-carbon respectively. The relationships between these three independent variables of modelling carbon stock (CPA, DBH, height) and dependent variable (carbon) were highly significant at 95% confidence level ($P<0.001$). A total of 637,119.87Mg carbon was estimated in the study area with an average of 185Mg C per hectare with a model accuracy of 84% and RMSE 29.3%. Thus the study found the technique to be promising and made the following conclusions to address the research questions:

How accurately CPA can be segmented from VHRS image?

Segmentation accuracy was evaluated using one to one matching of reference and segmented polygons and measure of goodness of fit (D-value). The resulted accuracy of segmentation using 1:1 and D-value was 72% and 68% respectively. The average achieved accuracy of this study was 70%.

Is there a significant difference between DBH and height derived from TLS and manual field measurement?

DBH derived from TLS and measured from field were highly correlated as the coefficient of determination was 0.96. Similarly the relationships of height measured from field and derived from TLS was also with R^2 of 0.75. The statistical F-test and t-test was performed. F-test and t-test indicated that there is no significant difference at 95% confidence level between mean of DBH and height measurements from TLS and field since the t- calculated was greater than t-critical. Therefore, the null hypothesis was rejected.

Is there a significant difference between DBH and height estimated from CPA and manual field measurement?

The study found weak correlation between DBH and height estimated from CPA and corresponding field measurements. The result of the t-test indicated that there is significant difference between estimated and field measured DBH and height since the t-calculated was smaller than t-critical. Therefore the null hypothesis is rejected.

Is there a (at 95% confidence level) significant relationship between DBH, height measured from TLS and CPA segmented from VHRS images?

Data obtained from TLS and high resolution image were correlated. The correlation coefficient of DBH-CPA and CPA-height was 0.88 (R^2=0.79) and 0.81(R^2=0.68) respectively. Test of Pearson correlation coefficient indicated that the relationships were highly significant ($P<0.001$). Therefore, the study found the relationship between DBH-CPA and Height-CPA as significant at 95% confidence level.

6.2. Recomendations

1. Even though it takes time, increasing number of scan could improve level and quality of scanned point cloud data and avoided missing tress.
2. Despite the difficulties, it is possible to acquire information such as DBH from TLS point cloud data however capturing absolute tree height can result in variability of measurement due to the dense branching with layers of canopy in tropical rainforest.
3. More research is needed to derive advanced forest parameters.

LIST OF REFERENCES

A. Hanis, A. Abu Hassan, A.T Nurita, S. C. M. . (2014). Community structure of termites in a hill dipterocarp forest of Belum – Temengor Forest Complex , Malaysia: emergence of pest species. *Raffles Bulletin Of Zoology*, *62*, 3–11.

Andersson, K., Evans, T. P., & Richards, K. R. (2008). National forest carbon inventories: policy needs and assessment capacity. *Climatic Change*, *93*(1-2), 69–101.

Antonio, B,. Valerio, A,. Heiko B,. Luca, Belelli, M., Martial B,. Michael, B,. Ron, H., Matthew, H., Matieu, H., Martin, Herold., Anthony, Janetos, B., Elizabeth L., Raphaël, M., Lars Gunnar Marklund, Hakan Olsson, Devendra Pandey, M. S., Christiane Schmullius, Reuben Sessa, Yosio Edemir Shimabukuro, R., & Valentini, M. W. (2009). Assessment of the status of the development of the standards for the Terrestrial Essential Climate Variables. *GTOS*, *67*, 30.

Asner, G. P. (2009). Tropical forest carbon assessment: integrating satellite and airborne mapping approaches. *Environmental Research Letters*, *4*(3), 034009.

Asner, G. P. (2011). Painting the world REDD: addressing scientific barriers to monitoring emissions from tropical forests. *Environmental Research Letters*, *6*(2), 021002.

Baker, D. J., Richards, G., Grainger, A., Gonzalez, P., Brown, S., DeFries, R., Stolle, F. (2010). Achieving forest carbon information with higher certainty: A five-part plan. *Environmental Science & Policy*, *13*(3), 249–260.

Baral, S. (2011). *Mapping Carbon Stock Using High Resolution Satellite Images In Sub-Tropical Forest Of Nepal.* MSc Thesis, University of Twente, Faculty of Geo-Information Science and Earth Observation (ITC), Enschede,The Netherlands. Retrieved on from http://www.itc.nl/Pub/Home/library/Academic_output/AcademicOutput.html?p=11&y=11&l=20

Basuki, T. M., van Laake, P. E., Skidmore, a. K., & Hussin, Y. a. (2009). Allometric equations for estimating the above-ground biomass in tropical lowland Dipterocarp forests. *Forest Ecology and Management*, *257*(8), 1684–1694.

Benz, U. C., Hofmann, P., Willhauck, G., Lingenfelder, I., & Heynen, M. (2004a). Multi-resolution, object-oriented fuzzy analysis of remote sensing data for GIS-ready information. *ISPRS Journal of Photogrammetry and Remote Sensing*, *58*(3-4), 239–258.

Benz, U. C., Hofmann, P., Willhauck, G., Lingenfelder, I., & Heynen, M. (2004b). Multi-resolution, object-oriented fuzzy analysis of remote sensing data for GIS-ready information. *ISPRS Journal of Photogrammetry and Remote Sensing*, *58*(3-4), 239–258.

Beucher, S. (1992). The watershed transformation applied to image segmentation. *SCANNING MICROSCOPY-SUPPLEMENT*, 1–26.

Bienert, A., & Maas, H. (2008). Methods For The Automatic Geometric Registration Of Terrestrial Laser Scanner Point Clouds In Forest Stands. *Dresden University of Technology, Institute of Phot Ogrammetry and Remote Sensing*, 6.

Bienert, A., Maas, H., & Scheller, S. (2006). Analysis Of The Informaton Content Of Terrestrial Laserscanner Point clouds for The Automatic Determination Of Forest Invontory Parameters.

ISPRS WG VIII/11 & EARSEL Joint Conference "3D Remote Sensing in Forestry", *8/11*(14-15 February), 1–7.

Bienert, A., Scheller, S., Keane, E., Mullooly, G., & Mohan, F. (2006). Application of Terrestrial Laser Scanners For The Determination Of Forest Inventory Parameters. *International Archives of Photogrammetry , Remote Sensing and Spatial Information Science*, *36*, 5.

Brandtberg, T., & Walter, F. (1998). Automated delineation of individual tree crowns in high spatial resolution aerial images by multiple-scale analysis. *Machine Vision and Applications*, *11*(2), 64–73.

Brown, S. (1997). *Estimating Biomass and Biomass Change of Tropical Forests: A Primer* (p. 55). FAO. Forestry paper 134, Rome.

Brown, S. (2002). Measuring carbon in forests: current status and future challenges. *Environmental Pollution*, *116*(3), 363–372.

Brown, S and Gaston, G. (1995). Use Of Forest Inventories And Geographic Information Systems To estimate Biomass Density Of Tropical forests: Application To Tropical Africa. *US Environmental Protection Agency*, *38*, 157–168.

Bryan, J., Shearman, P., Ash, J., & Kirkpatrick, J. B. (2010). Estimating rainforest biomass stocks and carbon loss from deforestation and degradation in Papua New Guinea 1972-2002: Best estimates, uncertainties and research needs. *Journal of Environmental Management*, *91*(4), 995–1001.

Bunting, P., & Lucas, R. (2006). The delineation of tree crowns in Australian mixed species forests using hyperspectral Compact Airborne Spectrographic Imager (CASI) data. *Remote Sensing of Environment*, *101*(2), 230–248.

Butler, R. (2012). Tropical Rainforests Of The World. Retrieved from http://rainforests.mongabay.com/0101.htm

C. Cosarca, A. Jocea, A. S. (2009). Analysis of error sources in terrestrial laser scanning. *RevCAD-Journal of Geodesy and Cadastre*, 115–123.

Cairns, M. A., Olmsted, I., Granados, J., & Argaez, J. (2003). Composition and aboveground tree biomass of a dry semi-evergreen forest on Mexico's Yucatan Peninsula. *Forest Ecology and Management*, *186*(1-3), 125–132.

Calders, K., Newnham, G., Burt, A., Murphy, S., Raumonen, P., Herold, M., Kaasalainen, M. (2014). Nondestructive estimates of above-ground biomass using terrestrial laser scanning. *Methods in Ecology and Evolution.*

Calders, K., Newnham, G., Herold, M., Murphy, S., Culvenor, D., Raumonen, P., … Disney, M. (2013). Estimating above ground biomass from terrestrial laser scanning in Australian Eucalypt Open Forest. *SILVIlASER*, 1–7.

Calders, K., Verbesselt, J., Bartholomeus, H., & Herold, M. (2011). Applying terrestrial LiDAR to derive gap fraction distribution time series during bud break. *University of Wageningen, Laboratory of Geo-Information Science and Remote Sensing, the Netherland*, 1–9.

Carleer, A. P., Debeir, O., & Wolff, E. (2005). Assessment of Very High Spatial Resolution Satellite Image Segmentations. *Photogrammetric Engineering Remote Sensing*, *71*(11), 1285–1294.

Chave, J., Andalo, C., Brown, S., Cairns, M. a, Chambers, J. Q., Eamus, D.,Yamakura, T. (2005). Tree allometry and improved estimation of carbon stocks and balance in tropical forests. *Oecologia*, *145*(1), 87–99.

Chave, J., Condit, R., Aguilar, S., Hernandez, A., Lao, S., & Perez, R. (2004). Error propagation and scaling for tropical forest biomass estimates. *Philosophical Transactions of the Royal Society of London. Series B, Biological Sciences*, *359*(1443), 409–20.

Chekole, S. D. (2014). Surveying with GPS , total station and terresterial laser scaner : a comparative study. *MSc Thesis :School of Architecture and the Built Environment, Royal Institute of Technology (KTH)*, (3131), 1–55.

Chye, L. K. (2010). Belum-Temengor Forest Complex , north peninsular Malaysia. *BirdingASIA*, *14*(February 2004), 15–22.

Clemens Reimann, Peter Filzmoser, Robert Garrett, R. D. (2008). Statistical Data Analysis Explained: Applied Environmental Statistics with R.

Clinton, N., Holt, A., Scarborough, J., Yan, L., & Gong, P. (2010). Accuracy Assessment Measures for Object-based Image Segmentation Goodness. *Photogrammetric Engineering and Remote Sensing*, *76*(3), 289–299.

Culvenor, D. S. (2002). TIDA : an algorithm for the delineation of tree crowns in high spatial resolution remotely sensed imagery. *Computers & Geosciences*, *28*(1), 33–44.

Dassot, M., Constant, T., & Fournier, M. (2011). The use of terrestrial LiDAR technology in forest science: application fields, benefits and challenges. *Annals of Forest Science*, *68*(5), 959–974.

Definiens. (2008). User Guide.

Definiens. (2012a). Reference Book.

Dhital, N. (2009). Reducing Emissions from Deforestation and Forest Degradation (REDD) in Nepal : Exploring the Possibilities. *Journal of Forest and Livelihood 8(1)*, *8*(1), 56–62.

Digital Globe. (2009). WorldView-2.Retrived from: *http://www.digitalglobe.com/sites/default/files/DG_WorldView2_DS_PROD.pdf*, (October), 1–2.

Dirocco, T. L. (2012). A Thorough Quantification of Tropical Forest Carbon Stocks in Malaysia. *Spring*, 1–18.

Doane, D. P., & Seward, L. E. (2011). Measuring Skewness : A Forgotten Statistic ?, *19*(2), 1–18.

Draguţ, L., Tiede, D., & Levick, S. R. (2010). ESP: a tool to estimate scale parameter for multiresolution image segmentation of remotely sensed data. *International Journal of Geographical Information Science*, *24*(6), 859–871.

Drake, J. B., Dubayah, R. O., Knox, R. G., Clark, D. B., Blair, J. B., & Rica, C. (2002). Sensitivity of large-footprint lidar to canopy structure and biomass in a neotropical rainforest. *Remote Sensing of Environment*, *81*, 378–392.

Dubayah, Ralph O., Drake, J. B. (2000). Lidar Remote Sensing for Forestry Applications. *Journal of Forestry*, *98*(3), 44–46.

Dulal, H. B., Shah, K. U., & Sapkota, C. (2012). Reducing emissions from deforestation and forest degradation (REDD) projects: lessons for future policy design and implementation. *International Journal of Sustainable Development & World Ecology*, *19*(2), 116–129.

Ekoungoulou, R., 1, 2, Averti, S., Ifo, & 2, 3. (2014). Tree Above - And Below - Ground Biomass Allometries for Carbon Stocks Estimation in Secondary Forest of Congo. *OSR Journal of Environmental Science*, *8*(4), 9–20.

Erikson, M. (2004). Species classification of individually segmented tree crowns in high-resolution aerial images using radiometric and morphologic image measures. *Remote Sensing of Environment*, *91*(3-4), 469–477.

Erikson, M. (2011). Segmentation of individual tree crowns in colour aerial photographs using region growing supported by fuzzy rules. *Canadian Journal of Forest Research*. Retrieved on February 2015 from http://www.nrcresearchpress.com

Fang, Z., & Bailey, R. L. (1998). Height–diameter models for tropical forests on Hainan Island in southern China. *Forest Ecology and Management*, *110*(1-3), 315–327.

FAO. (2010). *Global Forest Resources Assessment. Main Report.*

Gartner, G., Meng, L., & Peterson, M. P. (2008). *Estimation of optimal image object size for the segmentation of forest stands with multispectral IKONOS imagery* (p. 804).

Gibbs, H. K., Brown, S., Niles, J. O., & Foley, J. A. (2007). Monitoring and estimating tropical forest carbon stocks: making REDD a reality. *Environmental Research Letters*, *2*(4).

Gonzalez, P., Asner, G. P., Battles, J. J., Lefsky, M. a., Waring, K. M., & Palace, M. (2010). Forest carbon densities and uncertainties from Lidar, QuickBird, and field measurements in California. *Remote Sensing of Environment*, *114*(7), 1561–1575.

Gougeon, F. A., & Leckie, D. G. (2006). The Individual Tree Crown Approach Applied to Ikonos Images of a Coniferous Plantation Area. *Photogrammetric Engineering and Remote Sensing*, *72*(11), 1287–1297.

Gschwantner, T., Schadauer, K., Vidal, C., Lanz, A., Tomppo, E., Cosmo, L., Lawrence, M. (2009). Common Tree Definitions for National Forest Inventories in Europe, *43*(July 2008).

Gupta, J. (2012). Glocal forest and REDD+ governance: win–win or lose–lose? *Current Opinion in Environmental Sustainability*, *4*(6), 620–627.

Gupta, J., Olsthoorn, X., & Rotenberg, E. (2003). The role of scientific uncertainty in compliance with the Kyoto Protocol to the Climate Change Convention. *Environmental Science & Policy*, *6*(6), 475–486.

Haala, N., Reulke, R., Thies, M., & Aschoff, T. (2004). Combination Of Terrestrial Laser Scanning with High Resolution Panoramic Images For Investigations In Forest applications And Tree Species Recognition. *University Of Stuttgart, Institute For Photogrammetry and University Of Freiburg, Institute For Forest Growth, Germany*, 1–4.

Hajnsek, I., Kugler, F., Lee, S., Papathanassiou, K. P., & Member, S. (2009). Tropical-Forest-Parameter Estimation by Means of Pol-InSAR : The INDREX-II Campaign. *IEEE Transactions On Geoscience And Remote Sensing*, *47*(2), 481–493.

Hall, S. a., Burke, I. C., Box, D. O., Kaufmann, M. R., & Stoker, J. M. (2005). Estimating stand structure using discrete-return lidar: an example from low density, fire prone ponderosa pine forests. *Forest Ecology and Management*, *208*(1-3), 189–209.

Hamzah, H. (2012). Modeling of Tropical Forest Conversion to Oil Palm Expansion Using Area Production Model Modeling of Tropical Forest Conversion to Oil Palm Expansion Using Area Production Model. *University of Twente, Faculty of Geo-Information Science and Earth Observation (ITC), Enschede,The Netherlands.*, 74.

Hay, G. J., Blaschke, T., Marceau, D. J., & Bouchard, A. (2003). A comparison of three image-object methods for the multiscale analysis of landscape structure. *ISPRS Journal of Photogrammetry and Remote Sensing*, *57*(5-6), 327–345.

Hemery, G. E., Savill, P. S., & Pryor, S. N. (2005a). Applications of the crown diameter–stem diameter relationship for different species of broadleaved trees. *Forest Ecology and Management*, *215*(1-3), 285–294.

Hemery, G. E., Savill, P. S., & Pryor, S. N. (2005b). Applications of the crown diameter–stem diameter relationship for different species of broadleaved trees. *Forest Ecology and Management*, *215*(1-3), 285–294.

Hirata, Y., Tsubota, Y., & Sakai, A. (2009). Allometric models of DBH and crown area derived from QuickBird panchromatic data in Cryptomeria japonica and Chamaecyparis obtusa stands. *International Journal of Remote Sensing*, *30*(19), 5071–5088.

Hopkinson, C., Chasmer, L., Young-pow, C., & Treitz, P. (2004). Assessing forest metrics with a ground-based scanning lidar. *Canadian Journal of Forest Research*, *34*, 573–583. doi:10.1139/X03-225

Huang, H., Gong, P., Cheng, X., Clinton, N., & Cao, C. (2008). Forest structural parameter extraction using terrestrial LiDAR. *State Key Laboratory of Remote Sensing Science, Jointly Sponsored by the Institute of Remote Sensing Applications of Chinese Academy of Sciences and Beijing Normal.*

Hudak, A. T., Strand, E. K., Vierling, L. A., Byrne, J. C., Eitel, J. U. H., Martinuzzi, S., & Falkowski, M. J. (2012). Quantifying aboveground forest carbon pools and fluxes from repeat LiDAR surveys. *Remote Sensing of Environment*, *123*, 25–40.

Hunter, M. O., Keller, M., Vitoria, D., & Morton, D. C. (2013). Tree height and tropical forest biomass estimation. *Biogeosciences Discussions*, *10*(6), 10491–10529.

Husch, B., Beers, T. W., Kershaw, J. A., & Jr. (2003). *Forest Mensuration* (4th ed., p. 443). New Kersy, USA.

Ilyas, S. (2013). Allometric Equation and Carbon Sequestration of Acacia mangium Willd . in Coal Mining Reclamation Areas. *Civil and Environmental Research*, *3*(1).

IPCC. (2006). *IPCC Guidelines for National Greenhouse Gas Inventories* (pp. 1–678).

IPCC. (2007a). *Land Use, Land-Use Change and Forestry.*

IPCC. (2007b). *The Physical Science Basis* (p. 1007).

IPCC, 2007: Summary for Policymakers. In: Climate Change 2007: The physical Science Basis: Contribution of Working Groupe Ito the fourth Assesment Report of the IntergovernmentalPanel onClimate Change. Cambridge University Press, Cambrdge,United Kingdom and New York, NY, USA.

Jenkins, J. C., Chojnacky, D. C., Heath, L. S., & Birdsey, R. A. (2004). Comprehensive Database of Diameter-based Biomass Regressions for North American Tree Species. *USDA Forest Service*, 48.

Jennings, S. B., Brown, N. D., & Sheil, D. (1999). Assessing forest canopies and understorey illumination : canopy closure , canopy cover and other measures. *Forestry*, *72*(1), 60–73.

Johnson, B., Tateishi, R., & Hoan, N. (2012). Satellite Image Pansharpening Using a Hybrid Approach for Object-Based Image Analysis. *ISPRS International Journal of Geo-Information*, *1*(3), 228–241.

Kanninen, M., Brockhaus, M., Murdiyarso, D., Nabuurs, G. (2010). Harnessing forests for climate change mitigation through REDD+: challenges and opportunities. *Global Environmental Changes*, 43–54.

Karna, Y. K. (2012). Mapping Above Ground Carbon Using WorldView Satellite Image And Lidar Data In Relationship With Tree Diversity Of Forests. *University of Twente, Faculty of Geo-Information Science and Earth Observation (ITC), Enschede,The Netherlands.*, 94.

Katoh, M., Gougeon, F. a., & Leckie, D. G. (2008). Application of high-resolution airborne data using individual tree crowns in Japanese conifer plantations. *Journal of Forest Research*, *14*(1), 10–19.

Kaur, R,. Ong, T,. Lim, K, C,. Yeap, C, A. (2011). A Survey On Mass Movement Of The Vulnerable Plain-Pouched Horribill In The Belum-Tmenger Forest Complex, Peninsular Malaysia. *The Raffles Bulletin Of Zoology*, *24*, 171–176.

Kavzoglu, T., & Yildiz, M. (2014). Parameter-Based Performance Analysis of Object-Based Image Analysis Using Aerial and Quikbird-2 Images. *ISPRS Annals of Photogrammetry, Remote Sensing and Spatial Information Sciences*, *II-7*(October), 7.

Ke, Y., & and Quackenbush, L. J. (2008). Comparison Of Individual Tree Crown Detection And Delineation. *Paper Presented at the Proceedings of 2008 ASPRS Annual Conference, American Society of Photogrammetry and Remote Sensing.*

Ke, Y., & Quackenbush, L. J. (2011). Review Article A review of methods for automatic individual tree-crown detection and delineation from passive remote sensing. *International Journal of Remote Sensing*, *32*(17), 4725–4747.

Ketterings, Q. M., Coe, R., van Noordwijk, M., Ambagau', Y., & Palm, C. A. (2001). Reducing uncertainty in the use of allometric biomass equations for predicting above-ground tree biomass in mixed secondary forests. *Forest Ecology and Management*, *146*(1-3), 199–209.

Kim, M., Madden, M., & Warner, T. (2008). Estimation of optimal image object size for the segmentation of forest stands with multispectral IKONOS imagery. *Springer*, 291–307.

King, D. A., Davies, S. J., Supardi, M. N. N., & Tan, S. (2005). Tree growth is related to light interception and wood density in two mixed dipterocarp forests of Malaysia. *Functional Ecology*, *19*(3), 445–453.

Koch, B., Heyder, U., & Weinacker, H. (2006). Detection of Individual Tree Crowns in Airborne Lidar Data, *72*(4), 357–363.

Köhl, M., Baldauf, T., Plugge, D., & Krug, J. (2009). Reduced emissions from deforestation and forest degradation (REDD): a climate change mitigation strategy on a critical track. *Carbon Balance and Management*, *4*(1), 10.

Koji Shimano. (1997). Analysis of the Relationship between DBH and Crown Projection Area Using a New Model Koji Shimano 1. *Journal of Forest Research*, *2*, 237–242.

Korhonen, L., Korhonen, K. T., Rautiainen, M., & Stenberg, P. (2006). Estimation of Forest Canopy Cover : a Comparison of Field Measurement Techniques. *Silva Fennica*, *40*(4), 577–588.

Lamonaca, A., Corona, P., & Barbati, A. (2008). Exploring forest structural complexity by multi-scale segmentation of VHR imagery. *Remote Sensing of Environment*, *112*(6), 2839–2849.

Laumonier, Y., Edin, A., Kanninen, M., & Munandar, A. W. (2010). Landscape-scale variation in the structure and biomass of the hill dipterocarp forest of Sumatra: Implications for carbon stock assessments. *Forest Ecology and Management*, *259*(3), 505–513.

Lefsky, M. A., Cohen, W. B., Harding, D. J., Parker, G. G., Acker, S. A., Gower, S. T., Flight, S. (2002). Lidar remote sensing of above-ground biomass in three biomes. *Global Ecology and Biogeograhpyiogeograhpy*, *2*, 393–399.

Lefsky, M. a., Cohen, W. B., Parker, G. G., & Harding, D. J. (2002). Lidar Remote Sensing for Ecosystem Studies. *BioScience*, *52*(1), 19.

Li, Z., Hayward, R., Zhang, J., & Liu, Y. (2008). QUT Digital Repository : Individual Tree Crown Delineation Techniques for Vegetation Management in Power Line Corridor, (December), 1–3.

Liang, X. (2013). *Feasibility of Terrestrial Laser Scanning for Plotwise Forest Inventories* (pp. 1–55).

Liang, Xinlian, Paula Litkey, Juha Hyyppä, Harri Kaartinen, Kukko, Antero, M. H. (2011). Automatic Plot-Wise Tree Location Mapping Using Single-Scan Terr Estrial Laser Scanning. *The Photogrammetric Journal of Finland*, *22*(2), 37–48.

Lim, K., Treitz, P., Wulder, M., St-Onge, B., & Flood, M. (2003). LiDAR remote sensing of forest structure. *Progress in Physical Geography*, *27*(1), 88–106.

Litton, C. M., Ryan, M. G., Tinker, D. B., & Knight, D. H. (2003). Belowground and aboveground biomass in young postfire lodgepole pine forests of contrasting tree density. *NRC Research Press, Canada*, *363*, 351–363.

Lu, D. (2005). Aboveground biomass estimation using Landsat TM data in the Brazilian Amazon. *International Journal of Remote Sensing*, *26*(12), 2509–2525.

Lu, D. (2006). The potential and challenge of remote sensing‐based biomass estimation. *International Journal of Remote Sensing*, *27*(7), 1297–1328.

Maan, G. S., Singh, C. K., Singh, M. K., & Nagarajan, B. (2014). Tree species biomass and carbon stock measurement using ground based-LiDAR. *Geocarto International*, (7), 1–18.

Maas, H. ‐G., Bienert, a., Scheller, S., & Keane, E. (2008). Automatic forest inventory parameter determination from terrestrial laser scanner data. *International Journal of Remote Sensing*, *29*(5), 1579–1593.

MacKay, D. B., Wehi, P. M., & Clarkson, B. D. (2011). Evaluating restoration success in urban forest plantings in Hamilton, New Zealand. *Urban Habitats*, *6*(1).

Maharjan, S. (2012). *Estimation and Mapping Above Ground Woody Carbon Stocks Using Lidar Data And Digital Camera Imagery In The Hilly Forest Of Gorkha, Nepal.* MSc Thesis, University of Twente, Faculty of Geo-Information Science and Earth Observation (ITC), Enschede,The Netherlands., 70. Retrieved in from http://www.itc.nl/Pub/Home/library/Academic_output/AcademicOutput.html?p=11&y=12&l=20

Maxwell, T. and Y. Z. (2006). A Fuzzy Logic Approach To Supervised Segmentation For Object Oriented Classification. *ASPRS Annual Conference*, (1), 7.

McHale, M. R. (2008). Volume estimates of trees with complex architecture from terrestrial laser scanning. *Journal of Applied Remote Sensing*, *2*(1).

Means, J. E., Acker, S. A., Harding, D. J., Blair, J. B., Lefsky, M. A., Cohen, W. B., Mckee, W. A. (1999). Use of Large-Footprint Scanning Airborne Lidar To Estimate Forest Stand Characteristics in the Western Cascades of Oregon. *Remote Sensing of Environment*, *308*(April 1998), 298–308.

Mohren, G., Hasenauer, H., Köhl, M., & Nabuurs, G.-J. (2012). Forest inventories for carbon change assessments. *Current Opinion in Environmental Sustainability*, *4*(6), 686–695.

Möller, M., Lymburner, L., & Volk, M. (2007). The comparison index: A tool for assessing the accuracy of image segmentation. *International Journal of Applied Earth Observation and Geoinformation*, *9*(3), 311–321.

Moorthy, I., Miller, J. R., Hu, B., Chen, J., & Li, Q. (2008). Retrieving crown leaf area index from an individual tree using ground-based lidar data, *34*(3), 320–332.

Mora, B., Wulder, M. A., & White, J. C. (2010). Segment-constrained regression tree estimation of forest stand height from very high spatial resolution panchromatic imagery over a boreal environment. *Remote Se*nsing *of Environment*, *114*(11), 2474–2484.

Nguyet, D. A. N. H. (2012). *Error Propqgqtion In Carbon Estimation Using The Combination Of Airborne Lidar Data And Very High Resolution Geo-Eye Satellite Imagery In Ludhikhola Watershed, Gorkha, Nepal. MSc Thesis*, University of Twente, Faculty of Geo-Information Science and Earth Observation (ITC), Enschede,The Netherlands., 74. Retrieved in from http://www.itc.nl/Pub/Home/library/Academic_output/AcademicOutput.html?p=11&y=12&l=20

Noble, I. R., & Dirzo, R. (1976). Forests as Human-Dominated Ecosystems. *Science, 227(25)*

Okuda, T., Suzuki, M., Numata, S., Yoshida, K., Nishimura, S., Adachi, N., Hashim, M. (2004). Estimation of aboveground biomass in logged and primary lowland rainforests using 3-D photogrammetric analysis. *Forest Ecology and Management*, *203*(1-3), 63–75.

Olofsson, K., Holmgren, J., & Olsson, H. (2014). Tree Stem and Height Measurements using Terrestrial Laser Scanning and the RANSAC Algorithm. *Remote Sensing*, *6*(5), 4323–4344.

Padwick, C., Scientist, P., Deskevich, M., Pacifici, F., & Smallwood, S. (2010). Worldview-2 pan-sharpening. *Paper Presented at the ASPRS 2010 Annual Conference. San Diego, California.*

Pelletier, J., Kirby, K. R., & Potvin, C. (2012). Significance of carbon stock uncertainties on emission reductions from deforestation and forest degradation in developing countries. *Forest Policy and Economics*, *24*, 3–11.

Pelletier, J., Ramankutty, N., & Potvin, C. (2011). Diagnosing the uncertainty and detectability of emission reductions for REDD + under current capabilities: an example for Panama. *Environmental Research Letters*, *6*(2), 024005.

Pohl, C., & Genderen, J. L. V. A. N. (1998). Review article M ultisensor image fusion in remote sensing : concepts , methods and applications. *International Journal of Remote Sensing*, *19*(5), 823–854.

Ravindranath, N. H. M. O. (2008). Carbon Inventory Methods: Handbook for Greenhouse Gas Inventory, Carbon Mitigation and Roundwood Production Projects. *Springer*, *29*(149-156), 149–156.

Riegl. (2009). RIEGL VZ-400 Laser Scanners News. Retrived on February 2015 from *http://www.riegl.com/uploads/tx_pxpriegldownloads/RIEGL_VZ-400_News_03-2009.pdf*, (March), 1–8.

Riegl. (2013). RIEGL VZ-4000, 1–6. Retrieved on February 2015 from http://www.riegl.com/uploads/tx_pxpriegldownloads/10_DataSheet_VZ-4000_23-09-2013.pdf

Rosell, J. R., Llorens, J., Sanz, R., Arnó, J., Ribes-Dasi, M., Masip, J., Palacín, J. (2009). Obtaining the three-dimensional structure of tree orchards from remote 2D terrestrial LIDAR scanning. *Agricultural and Forest Meteorology*, *149*(9), 1505–1515.

Rote, R. G. (2003). Estimation of crown radii and crown projection area from stem size and tree position. *ANNUALS of FOREST SCIENCE*, *60*, 393–402.

Rutishauser, E., Noor'an, F., Laumonier, Y., Halperin, J., Hergoualc'h, K., & Verchot, L. (2013). Generic allometric models including height best estimate forest biomass and carbon stocks in Indonesia. *Forest Ecology and Management*, *307*, 219–225.

Ryherd, S., & Woodcock, C. (1996). Combining Spectral and Texture Data in the Segmentation of Remotely Sensed Images. *Photogrammetric Engineering & Remote Sensing*, *62*, 181–194.

Schwartzman, P. M. & S. (2005). Tropical Deforestation and Climate Change. *Institute for Environmental Research*, 132.

Seidel, D. (2011). Terrestrial laser scanning Applications in forest ecological research. *Göttingen Centre for Biodiversity and Ecology*, *6*, 145.

Shah, S. K. (2011). *Modelling The Relationship Between Tree Canopy Projection Area And Above Ground Carbon Stock Using High Resolution GeoEye Satellite Images*. MSc thesis, University of Twente, Faculty of Geo-Information and Earth Observation Science (ITC), Enschede, The Netherlands., 93. Retrieved in from http://www.itc.nl/Pub/Home/library/Academic_output/AcademicOutput.html?p=11&y=11&l=20

Simone Aparecida Vieira, Luciana Ferreira Alves, Marcos Aidar, L. S. A., Tim Baker, João Luís Ferreira Batista, Mariana Cruz Campos, P. B. C., Jerome Chave, Welington Braz Carvalho Delitti, Niro Higuchi, E. H., & Carlos Alfredo Joly, Michael Keller, Luiz Antonio Martinelli, Eduardo Arcoverde de Mattos, Thiago Metzker, Oliver Phillips, Flavio Antonio Maes dos Santos, Mônica Takako Shimabukuro, M. S. & S. E. T. (2008). Estimating Biomass and Biomass Change of Tropical Forests: A Primer. *Primer (FAO Forestry Paper-134)*, *8*(2), 21–29.

Simonse, M., Aschoff, T., Spiecker, H., & Thies, M. (2003). Automatic Determination Of Forest Inventory Parameters Using Terrestrial Laser Scanning. *University Of Freiburg, Insstitute of Forest Growth, Germany*, 1–7.

Singh, N. (2014). Impact Of Infestation Of Sal Heartwood Borer (Hoplocerambyx Spinicornis) On The Carbon Stock Of Sal (Shorea Robusta) Forests Of Doon Valley. MSc Thesis*, Indian Institute of Remote Sensing*, 57.

Song, C., Dickinson, M. B., Su, L., Zhang, S., & Yaussey, D. (2010). Estimating average tree crown size using spatial information from Ikonos and QuickBird images: Across-sensor and across-site comparisons. *Remote Sensing of Environment*, *114*(5), 1099–1107.

Sumarah, A. D. W. I. (2014). *A Combination Of Computer Vision And Object Based Image Segmentation To Model Forest Biomass And Carbon Stock In Tropical Rain Forest Of Kelay , Indonesia A Combination Of Computer Vision And Object Based Image Segmentation To Carbon Stock In Tropical Raian Forest of Kelay Indonesia*. MSc Thesis, University of Twente, Faculty of Geo-Information Science and Earth Observation (ITC), Enschede,The Netherlands.,69. Retrieved in from http://www.itc.nl/Pub/Home/library/Academic_output/AcademicOutput.html?p=11&y=11&l=20

Temesgen, H., Lemay, V., & Mitchell, S. J. (2005). Tree crown ratio models for multi-species and multi-layered stands of southeastern British Columbia. *THE FORESTRY CHRONICLE*, *81*(1), 133–141.

Thies, M., Spiecker, H., & Str, T. (2004). Evaluation And Future Prospects Of Terrestrial Laser Scanning For Standardized Forest Inventories. *International Archive of Photogrammetry, Remot Sensing and Spatial Information Sciences*, *36*, 192–197.

Tsendbazar, N. (2011). *Object Based Image Analysis Of Geo-Eye VHR Data To Model Obove Ground Carbon Stock In Himalayan Mid-Hill Forests, Nepal*. University of Twente, Faculty of Geo-Information Science and Earth Observation (ITC), Enschede,The Netherlands.,74. Retrieved in from http://www.itc.nl/Pub/Home/library/Academic_output/AcademicOutput.html?p=11&y=11&l=20

UNFCCC. (1998). Kyoto Protocol To The United Nations Framework Convention On Climate Change. *UNFCCC Secretatiatat, Bonn*, 21.

Vaglio Laurin, G., Chen, Q., Lindsell, J. A., Coomes, D. A., Frate, F. Del, Guerriero, L.,Valentini, R. (2014). Above ground biomass estimation in an African tropical forest with lidar and hyperspectral data. *ISPRS Journal of Photogrammetry and Remote Sensing*, *89*, 49–58.

Van de Geer, S., & Wegkamp, M. (Eds.). (2012). *Selected Works of Willem van Zwet*. New York, NY: Springer New York. doi:10.1007/978-1-4614-1314-1

Wang, C. (2006). Biomass allometric equations for 10 co-occurring tree species in Chinese temperate forests. *Forest Ecology and Management*, *222*(1-3), 9–16.

Wang, G., Gertner, G. Z., Fang, S., & Anderson, A. B. (2005). A Methodology for Spatial Uncertainty Analysis Of Remote Sensing and GIS Products. *Photogrammetric Engineering & Remote Sensing*, *71*(12), 1423–1432.

Wang, L., Gong, P., & Biging, G. S. (2004). Individual Tree-Crown Delineation and Treetop Detection in High-Spatial-Resolution Aerial Imagery. *Photogrammetric Engineering & Remote Sensing*, *3114*(March), 351–358.

Waring, R. H., Way, J., Hunt, E. R. J., Morrissey, L., Ranson, K. J., Weishampel, J. F., Franklin, S. E. (1995). Imaging radar for ecosystem studies.

Watt, P. J., & Donoghue, D. N. M. (2005). Measuring forest structure with terrestrial laser scanning. *International Journal of Remote Sensing*, *26*(7), 1437–1446.

Wei, W., Chen, X., & Ma, A. (2005). Object-oriented Information Extraction and Application in High-resolution Remote Sensing Image. *IEEE*, (C), 5–8.

Wright, S. J. (2005). Tropical forests in a changing environment. *Trends in Ecology & Evolution*, *20*(10), 553–60.

WWF. (2014). WWF Malaysia, Royal Belum State Park, Perak. Retrieved on Feburary 2015 from http://www.wwf.org.my/about_wwf/what_we_do/forests_main/forest_protect/protect_projects/project_royal_belum/

Zhan, Q., Molenaar, M., Tempfli, K., & Shi, W. (2005). Quality assessment for geo-spatial objects derived from remotely sensed data. *International Journal of Remote Sensing*, *26*(14), 2953–2974.

Zheng, G., Chen, J. M., Tian, Q. J., Ju, W. M., & Xia, X. Q. (2007). Combining remote sensing imagery and forest age inventory for biomass mapping. *Journal of Environmental Management*, *85*(3), 616–23.

LIST OF APPENDICES

Appendix 1: Histogram of CPA from image for the observations used for modelling carbon stock.

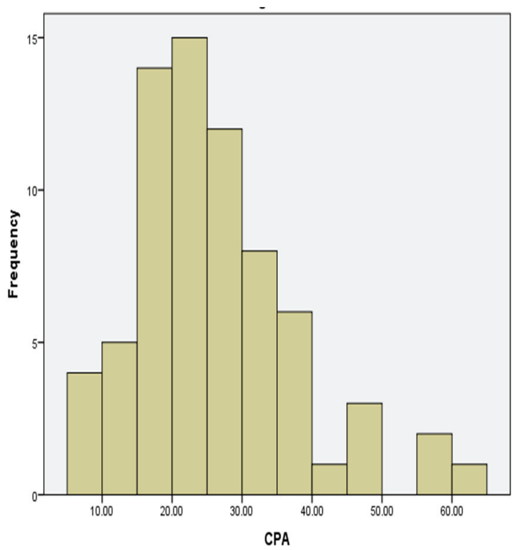

Appendix 2: Collinearity test of CPA and height used for multiple regression model

Coefficients[a]

Model		Collinearity Statistics	
		Tolerance	VIF
1	TLS_height	.316	3.167
	CPA	.316	3.167

a. Dependent Variable: Carbon

Appendix 3: Histogram of 586 DBH observations measured manually in field

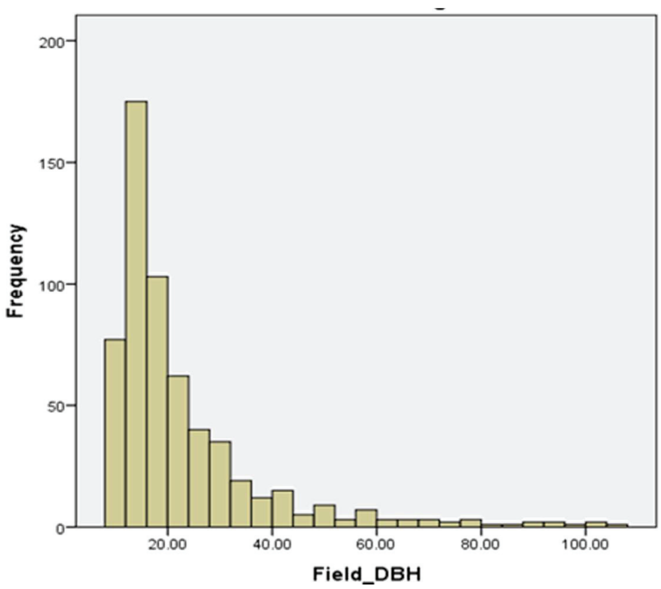

Appendix 4: Histogram of 586 height observations measured manually in field

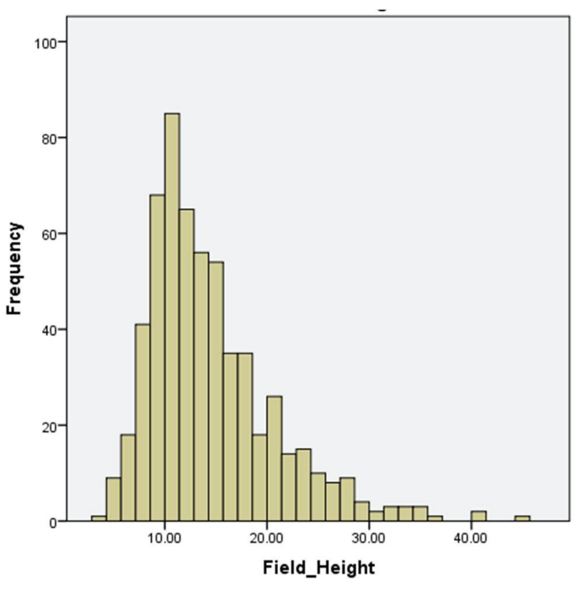

Appendix 5: Field data collection sheet used for the study

Plot No.: Date: Time: Name of Recorder:

Reference Point: Bearing: Distance:

Slope (%): Aspect: FCD Class No. Average:

Centre Position: X-Coordinate: Y-Coordinate: Z-coord.:

Scan Positions: 1.

S. N.	X-Coord	Y-coord	Z-coord	DBH (cm)	Height (m)	CD(m)	Species	Remarks

Appendix 6: TLS metadata used to collect details of every scan position in every plot

Plot details				coordinates		Scan details					
Plot. no	Slope	FCD	Scan. no	x	y	Form	resolution	Date	Time	Scan position	Remark

Appendix 7: Slope correction table used in field

Slope%	Radius(m)	Slope%	Radius(m)	Slope%	Radius(m)
0	12.62				
1	12.62	36	13.01	71	13.97
2	12.62	37	13.03	72	14.00
3	12.62	38	13.05	73	14.04
4	12.62	39	13.07	74	14.07
5	12.62	40	13.09	75	14.10
6	12.63	41	13.12	76	14.14
7	12.63	42	13.14	77	14.17
8	12.64	43	13.16	78	14.21
9	12.64	44	13.19	79	14.24
10	12.65	45	13.21	80	14.28
11	12.65	46	13.24	81	14.31
12	12.66	47	13.26	82	14.35
13	12.67	48	13.29	83	14.38
14	12.68	49	13.31	84	14.42
15	12.69	50	13.34	85	14.45
16	12.70	51	13.37	86	14.49
17	12.71	52	13.39	87	14.52
18	12.72	53	13.42	88	14.56
19	12.73	54	13.45	89	14.60
20	12.74	55	13.48	90	14.63
21	12.75	56	13.51	91	14.67
22	12.77	57	13.53	92	14.71
23	12.78	58	13.56	93	14.74
24	12.79	59	13.59	94	14.78
25	12.81	60	13.62	95	14.82
26	12.82	61	13.65	96	14.85
27	12.84	62	13.68	97	14.89
28	12.86	63	13.72	98	14.93
29	12.87	64	13.75	99	14.97
30	12.89	65	13.78	100	15.00
31	12.91	66	13.81	101	15.04
32	12.93	67	13.84	102	15.08
33	12.95	68	13.87	103	15.12
34	12.97	69	13.91	104	15.15
35	12.99	70	13.94	105	15.19

Source: Y.A. Hussin (2001) from lecture note

Appendix 8: whole image segmented in eCognition software.

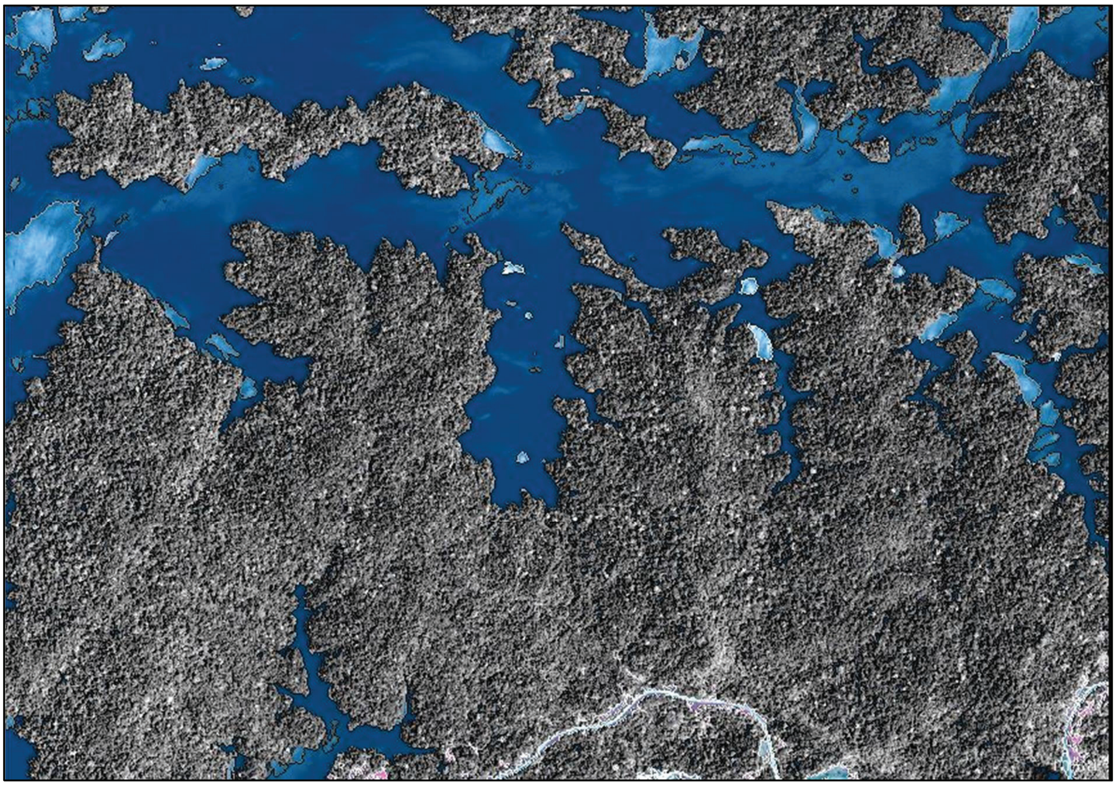

Appendix 9: Pearson correlation test of Field and TLS measurements

Correlations test of Field and TLS DBH

		fdbh	tdbh
fdbh	Pearson Correlation	1	.961**
	Sig. (2-tailed)		.000
	N	586	586
tdbh	Pearson Correlation	.961**	1
	Sig. (2-tailed)	.000	
	N	586	586

**. Correlation is significant at the 0.01 level (2-tailed).

Correlations test of Field and TLS height

		fheight	theight
fheight	Pearson Correlation	1	.859**
	Sig. (2-tailed)		.000
	N	586	586
theight	Pearson Correlation	.859**	1
	Sig. (2-tailed)	.000	
	N	586	586

**. Correlation is significant at the 0.01 level (2-tailed).

Appendix 10: Photos of the field work and study area